T U M

I N S T I T U T F Ü R I N F O R M A T I K

Signaling direction of motion at the output of retina. From biophysics of neural computation to computational models

Aurel V Martiniuc and Alois Knoll

TUM-I1002
Februar 10

T E C H N I S C H E U N I V E R S I T Ä T M Ü N C H E N

TUM-INFO-02-I1002-0/1.-FI

Druck: Institut für Informatik der
Technischen Universität München

Technical Report

Signaling direction of motion at the output of retina.
From biophysics of neural computation to computational models.

Aurel Vasile Martiniuc and Alois Knoll

Robotics and Embedded Systems, Computer Science Department,
Technical University of Munich, Germany
September, 2009

Abstract. The estimation of motion direction from time varying images is a fundamental task of both biological and artificial visual systems. Directional selective neurons are found in all species; moreover, in many of them, direction of motion is signaled already at the output of retina being carried to higher brain areas. Here we use simple schemes to investigate how directional selectivity changes for cells postsynaptic to retinal neurons. We show how sharpening in directional selectivity is achieved at the output of retina. The goal of this work is to infer from biophysics of neural computation and build computational models to account for direction of visual stimulus motion. A compromise between biological plausibility and computational efficacy is ubiquitous. However, the dimension of this compromise is an issue of scientific debate.

Contents

1. Introduction to basics of neural computation …. 4

2. Early Visual System. Direction selectivity …. 17

3. Sharpening in direction selectivity at the output of retina …. 30

4. Descriptive model for ON-OFF DSRGC RF characterization …. 62

1. Introduction to basics of neural computation

Recently increasing amount of scientific efforts is dedicated to bring together two distinct scientific approaches consisting in biophysics of neurons and information processing. Investigating how neurons process information one must consider both aspects, ionic channels, synapses, dendrites, axons, neurons and computation that they perform, i. e. multiplications in dendritic tree of a neuron.

Neurons are unique in their capability to edit and propagate signals very fast over fairy large distances. To do this, they generate typical electrical pulses known as action potentials in response to chemical or other impulses, which propagate along the nerve fibers (axons) toward other cells. The dendritic tree allows a neuron to receive inputs from many other neurons through synaptic connections. Along with these morphological features, neurons have physiological specializations i.e. a large variety of membrane-spanning ion-channels that selectively allow ions to move into or out of the cell. Perhaps one of the most sophisticated stochastic computational mechanisms consists in the manner in which ionic channels control the flow of ions across the cell membrane by opening and closing in response to voltage changes. The electrical signal of relevance to the nervous system is the difference in electrical potential between the inside and outside of a cell. Resting membrane potential (the potential at equilibrium maintained by ion pumps in the cell membrane) is known to be negative as compared with extracellular medium. Current in the form of charged ions flowing into or out of the cell through ionic channels will depolarize (less negative) or hyperpolarize (more negative) the membrane potential. If a neuron is depolarized sufficiently to

raise the membrane potential above the threshold level the neuron generates an action potential. Action potential generation however, depends on the history of cell firing in the sense that for a few milliseconds after an action potential was fired there is a refractory period during which there is impossible for the cell to fire another action potential. While action potentials are the only membrane potential fluctuations capable to propagate over large distances, there are also subthreshold potential fluctuations which are severely attenuated over relatively small distances. The mechanism through which neurons commonly communicate continues with the synaptic cleft – the place where axons terminates at synapses, where the voltage transient of the action potential opens ion channels producing an influx of Ca 2+ that leads to release of neurotransmitter. The neurotransmitter binds to the specific appropriate receptor at the postsynaptic side and open ion conducting channels. Depending on the nature of the ion flow, the synapses can have an excitatory (depolarizing) effect or an inhibitory (hyperpolarizing) effect at the postsynaptic level.

Because action potentials are abrupt changes in membrane potential, they can be detected by measuring the current just outside of a neuron's soma or axon (extracellular recording). The individual spikes last for only a few milliseconds, with most of the structure being confined to an even smaller window of time. It is useful to treat the spikes as instantaneous events that can be characterized completely by the time at which they occur.

Typically neurons respond to a given stimulus by producing complex spike sequences that reflect both the intrinsic dynamics of the neuron and temporal characteristics of the stimulus. Neural responses can vary from trial to trial even if the same stimulus is presented repeatedly. The complexity and variability of spike trains do not allow us to characterize them deterministically. As a consequence, models that can account for the probabilities that different spike sequences are evoked by specific stimulus are usually sought.

Basic spike train statistics

Firing Rate

A spike train containing n neurons can be represented as a sequence of times at which each spike occurs ti where i = 1, 2, ..., n on the interval 0 <= ti <= T.

The neural response function r(t) is a sum of Dirac delta functions located at points defined by the spike times:

$$r(t) = \sum_{i=1}^{n} \delta(t - t_i)$$

If we define Dirac delta function :

$$\int_0^T r(t) d\tau = n$$

And calculate the spike count rate as r = n/T , then :

$$r = \frac{1}{T} \int_0^T r(\tau) d\tau$$

Time dependent firing rate represents the average number of spikes appearing during a short time interval divided by the duration of the interval.

Spike Triggered Average

Ideally, a neuron will respond primarily to a single physical feature of a presented stimulus. The significant feature can be expressed as a time dependent variable s(t), and the other attributes of the stimulus can be ignored. For each spike time ti there is a corresponding section of the stimulus, s(ti − τ), which begins a certain time before the spike occurs. The spike triggered average (STA), written C(τ), is the average of each of these stimulus segments:

$$C(\tau) = \frac{1}{n}\sum_{i=1}^{n} s(t_i - \tau)$$

Reverse Correlation Function

The STA can also be expressed in the form of an integral by utilizing the conveniently defined neural response function.

$$C(\tau) = \frac{1}{n}\int_{0}^{T} r(t)s(t-\tau)dt$$

The integral form of C(τ) is particularly useful if we note that the crosscorrelation of r(t) and s(t), which are both real functions, is defined as:

$$Q_{rs}(\tau) = \frac{1}{T}\int_{0}^{T} r(t)s(t+\tau)dt$$

The relationship given by combining last two equations:

$$C(\tau) = \frac{n}{T} Q_{rs}(-\tau)$$

Because of the argument of the correlation function is negative, the STA is often called the reverse correlation function and it is proportional to the correlation of the firing rate with the stimulus at preceding times.

The results obtained by STA depend on the particular set of stimuli used during the experiment. To find a more accurate correlation it is the best choice to use a stimulus that is uncorrelated from one time to the next. In this way we can sample the neural response to stimulus fluctuations at all frequencies with equal weight. White noise stimulus has the defining characteristic that its value at any time is uncorrelated with its value at any other time (equal power at any frequencies).

Autocorrelation function of any stimulus is:

$$Q_{ss} = \frac{1}{T} \int_0^T s(t)s(t+\tau)dt$$

For white noise stimulus the autocorrelation function is 0 in the range $-T/2 < \tau < T/2$ except when $\tau=0$ and for this value $Q_{ss} = \sigma_s^2 \delta(\tau)$, where σ_s which has the units of stimulus times the square root of unit time, reflects the magnitude of the variability of the white noise.

The STA is a standard way of characterizing the selectivity of a neuron. The STA and reverse correlation can be used to construct linear estimates of firing rates evoked by arbitrary time dependent stimulus. These techniques have been used extensively to characterize properties of visually responsive neurons in early visual system: retina – LGN -V1. However, complex cells in V1 and neurons in higher areas (V2, etc) have more complex and nonlinear features in their visual responses which can not be captured by these linear techniques.

The activity of a neuron at time t depends on the behavior of stimulus over a period of time of several hundreds of milliseconds before t. Using reverse correlation method one address the problem of finding the estimate of firing rate rest(t) evoked by stimulus s(t). In a simple manner one can construct rest(t) as a weighted sum of stimulus intensity values taken at times prior t :

$$rest(t) = r_0 + \int_0^{\infty} D(\tau)s(t-\tau)d\tau$$

First term accounts for the background activity when stimulus s=0. This integral is a linear filter in which the kernel D(τ) shows how strong and with which sign the intensity value of the stimulus at time t- τ affects the firing rate at time t. This linear estimate represents first two terms in Volterra expansion in powers of stimulus. D(τ) is called the first order Wiener kernel, or simply the Wiener kernel, after Norbert Wiener, whose modifications of the Volterra expansion made it easier to use. According to the last equation, the relationship between r(t) and s(t) can be estimated using only the function D(τ). If this kernel can be calculated, then it is possible to reproduce or predict the response to a given stimulus. To construct an accurate firing rate estimate one has to optimize the kernel by minimizing the squared difference between estimated response and recorded response. This optimal kernel will be found solving the equation:

$$\partial E / \partial D = 0 \text{ and } E = \frac{1}{T}\int_0^T dt(rest(t) - r(t))^2$$

It is already known that for such a stimulus as white noise the optimal kernel that provides the best linear estimation of the firing rate is :

$$D(\tau) = \frac{Q_{rs}(-\tau)}{\sigma_s^2} = \frac{n}{T}\frac{C(\tau)}{\sigma_s^2}$$

Consequently, the best method to find the optimal kernel which to describe the linear response of a neuron is to calculate the STA in response to white noise stimulus.

Unfortunately the method described above fails when it has to predict highly nonlinear responses of some neurons. An improvement consists in adding some static nonlinearities to the linear estimate of the firing rate which to prevent firing rate to become negative and / or to account for the well known property of neuronal response saturation with stimulus increase. These static nonlinearities are known as threshold operation and saturation.

Thus a nonlinear function of linearly filtered stimulus is usually added:

$$L(t) = \int_0^\infty d\tau D(\tau) s(t-\tau)\,;\; rest(t) = r_0 + F(L(t))$$

The function F can be fitted using recorded data and should not allow firing rate estimate to become neither unrealistically large nor negative. Finally, a complete linear model to predict the spike trains of a particular type of neurons in response to a stimulus can be constructed using the firing rate estimate as described above to drive a stochastic spike generator. Using Poisson spike generator spikes are generated by comparing spiking probability in a small time interval r(t)Δ(t) with a random threshold.

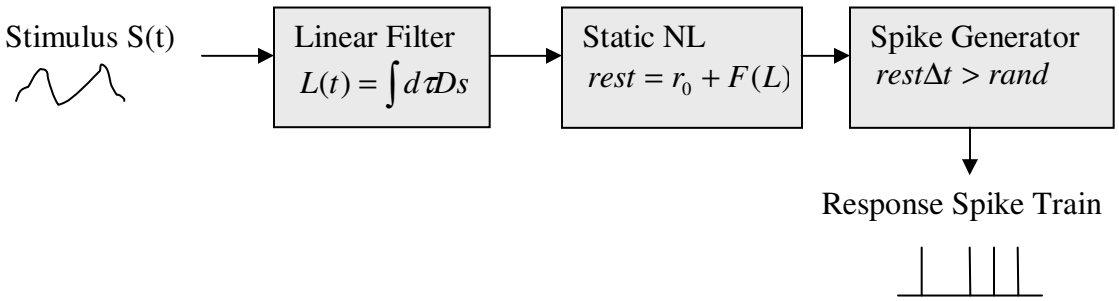

Descriptions of visual responses based on reverse correlation technique are approximate and they do not explain how visual responses arise from synaptic, cellular, and network properties of retinal, LGN and cortical circuits. For this purpose biophysics of neural computation must be taken into account. A very brief introduction to bioelectricity is therefore necessary.

All neurons are bounded by an insulating membrane that separates the electrochemical compartment inside the cell from the surrounding extracellular space. An electric potential exists across the cellular membrane due to the difference in the distribution of ions between the inside and the outside of the neuron. Te cell membrane is a lipid bilayer acting as a capacitor being impermeable to majority of the charged molecules. Trans-membrane proteins play an important role by closing and opening ion channels in response to environmental stimuli and thus modulate membrane potential. Due to the fact that the probability for these channels to be opened or closed depends on membrane potential they are known as voltage-gated channels. Many of the channels are highly selective allowing only one type of ions to pass through. When a neuron is inactive inside the membrane is an excess of negative charges so that at rest, the membrane (equilibrium) potential is negative. At this state, the flow of ions into the cell matches the flow out of the cell. This equilibrium can be disturbed by opening or closing ionic channels and thus membrane potential will fluctuate as well. Potential differences between different parts of a neuron cause ions to move within the cell. The intracellular medium provides resistance to such a flow. The intracellular resistivity can be also used to crudely estimate the conductance of a single channel. Neurons that have relatively negligible spatial variations in membrane potential it is known as electrotonically compact and they can be described by a single membrane potential. In this condition the membrane capacitance (Cm) is related to the membrane potential and to the amount

of charge Q by standard equation Q=CmV and explains how much current it is needed to change the membrane potential at a given rate (dQ/dt). The basic time scale for changes in membrane potential is set by membrane time constant (τm =RmCm). When the equilibrium state is achieved the net flow of the ions will be zero. The particular potential that satisfies the balancing conditions is

$E = \frac{V_T}{z} \ln(\frac{[IonConcentrationOutside]}{[IonConcentrationInside]})$, which is also known as Nernst equation and it applies for channels that allows only one single type of ions to pass through them. Some channels are not selective and in this case E takes intermediate values between equilibrium potentials of the individual ion types that pass through and it is called reversal potential. A conductance with reversal potential E tends to move the membrane potential of the neuron toward value of E. Thus, positive reversal potentials (i.e. Na+, Ca2+) tend to depolarize a neuron while negative reversal potentials (i.e. K+) tends to hyperpolarize the neuron. A conductance with E near resting potential will conduct little net current but they have another important effect, that is, to change membrane resistance of the neuron. This is called a shunting conductance. In the same manner, a synaptic conductance is also called excitatory or inhibitory based on its reversal potential values. Synapses with reversal potentials lower than the threshold value of membrane potential for generating an action potential are called inhibitory while synapses with reversal potential higher than the threshold are called excitatory.

The total current that flows across the membrane through all of its channels is called membrane current of the neuron and is quantified by summing currents due to all of the different types of channels including voltage-gated or synaptic channels. The difference between membrane potential and reversal potential (for a particular type of channel) is called the driving force. Summing over all different type of channels we have total membrane current:

$I = \sum_i g_i (V - E_i)$, where factor gi represents the conductance due to these channels.

While a membrane conductance changes over time, there are some factors that are constant contributing to the membrane current and they are called leakage currents. These are typically, the ion pumps currents to maintain the equilibrium nonzero: $I_l = g_l (V - E_l)$. The values of leakage conductance and resting potentials are usually specific to the cell that is being modeled.

A neuron will typically fire an action potential when its membrane potential is above a threshold value. During the action potential, the membrane potential follows a rapid, stereotyped trajectory and then returns to a value that is hyperpolarized relative to the threshold potential. In the constraints of single-compartment model (membrane potential is treated as a single variable) the efforts are focused to describe how charges flow into and out of a neuron and affect its membrane potential. Our present day understanding and methods of modeling neural excitability have been significantly influenced by the landmark work of Hodgkin and Huxley in which they unveiled the key properties of a ionic conductance underlying the nerve action potential. Their model accurately describes the stochastic manner in which different voltage-dependent conductances produce action potentials. Presumably, the HH model represents the closest attempt to describe and predict at a biophysically plausible level the manner in which information is edited at single neuron level. On the other hand models can be simplified and still capture neuronal response for most of the neurons. In this manner simulations can be dramatically accelerated it's true in detriment of less biological plausibility. However, there are scientific hypothesis which definitely can be verified involving simpler approaches and still remain accurate. Integrate and fire neuron models are a valuable tool to perform this task. Endowed with specific synaptic conductances this simple model becomes a powerful tool to investigate information processing. Basic integrate and fire model assumes that an action potential is fired whenever the membrane potential reaches a threshold

value Vh. After the action potential, the membrane potential is reset to a value below the threshold potential. If the details of an action potential generation processes are not important for a particular modeling goal, the membrane current is modeled in as much details as is necessary.

Synaptic transmission at a spike mediated chemical synapse begins when an action potential invades the presynaptic terminal and activates voltage dependent Ca2+ channels. This causes vesicles containing transmitter molecules to fuse with the cell membranes and release their contents into synaptic cleft between the pre- and postsynaptic sides of the synapse. The transmitter molecules then bind to appropriate receptors of postsynaptic neuron and leads to opening of ion channels that modifies the conductance of postsynaptic neuron.

There are two classes of synaptic conductances that are distinguished by whether the transmitter binds to the synaptic channel and activates it directly, or the transmitter binds to a distinct receptor that activates the conductance indirectly. First type of synaptic conductance is called ionotropic and activates more rapidly than the second class called metabotropic. A synaptic conductance can be excitatory (glutamate neurotransmitter) or inhibitory (GABA). For the excitatory synapse receptor types are AMPA (fast activating and deactivating) and NMDA (considerably slower). GABA activates two important inhibitory synaptic conductances in the brain. GABAa (fast ionotropic) GABAb (slower metabotropic). Synaptic inputs can be incorporated in Integrate and fire neuron model by adding to the passive elements, the synaptic conductance specific for the particular goal of the modeling. A variant of classic I&F model is built by adding an excitatory synaptic conductance, an inhibitory synaptic conductance and an afterhyperpolarization conductance in order to take into account the refractory period. This conductance will control the membrane potential time course to the resting potential.

The membrane potential $V(t)$ of the I&F neuron is governed by

$$C_m \frac{dV}{dt} = -(V - V_{\text{rest}}) g_m - (V - E_a) \sum_f g_a (t - t_f) - (V - E_e) \sum_s g_e (t - t_s)$$

An action potential is generated whenever the membrane reaches the threshold V_{thresh}.

The first term on the right side of the equation describes the leakage current while the second term describes the effect of afterhyperpolarization (AHP) following each action potential. The input of the neuron is provided through excitatory channels (third term on right side) resulting in excitatory postsynaptic potentials (EPSPs). In the same manner inhibitory conductances can be added as well.

A time-dependent conductance is modeled using "alpha-function":

$$g_X(t) = \begin{cases} g_{\max,X} \frac{t}{\tau_X} e^{1-\frac{t}{\tau_X}}, & t \geq 0 \\ 0, & t < 0 \end{cases} \qquad X \in \{a, e, i\}$$

And membrane time constant given by

$\tau_m = g_m^{-1} C_m$, where τ_m represents the membrane time constant, g_m is the membrane conductance and C_m is the membrane capacitance.

Up to know we saw aspects of the basics of neural computations from both point of view – computational neuroscience and biophysics of neural computation. Computational models are trying to handle with the manner in which neurons encode and/or decode information within the nervous system using statistics to contribute to infer robust engineering solutions from the spectacular and most efficient manner of nervous system capacity to deal with different issues, and to transform them in computational models able to help us in information processing. From the biophysical point of view the degree of complexity moves toward descriptive models. How synaptic connections are functioning, how important plasticity is, what scale to use, single cell or neural network or for example how spike timing is supported by neurobiology? We sought a

simple manner to decipher how information is processed within nervous system, a compromise between the randomness and high non-linearity introduced by biological systems and pragmatism that engineering is feed with in order to achieve successfully functional systems which can not afford errors in performing their tasks.

2. Early Visual System. Direction Selectivity.

First stages in visual system are represented by retina, lateral geniculate nucleus (LGN) and primary visual cortex. Visual information is firstly encoded in trains of action potentials at the output of retina by one type of retinal cells type called retinal ganglion cells. Their axons are grouped together and leave retina through optic disc passing through optic chiasm and ending (mostly) in LGN. Excitatory and inhibitory synapses (of a high degree of complexity) are then formed in both directions between LGN and primary visual cortex. (Fig.1)

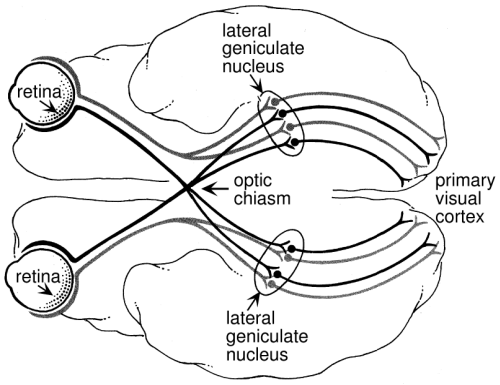

Fig.1 Stages of early visual system. Axons of retinal ganglion cells form optic nerves and carry on visual information through the optic chiasm mainly in to the lateral geniculate nucleus. From lateral geniculate nucleus visual information is further on processed in to the primary visual cortex (Adapted from Dayan and Abbott,2001).

Information flow through the retina following a direct path, from light receptors to bipolar cells to ganglion cells, and an indirect path, in which horizontal cells may be interposed between the receptors and bipolars, and amacrine cells between bipolars and retinal ganglion cells.(Fig.2)

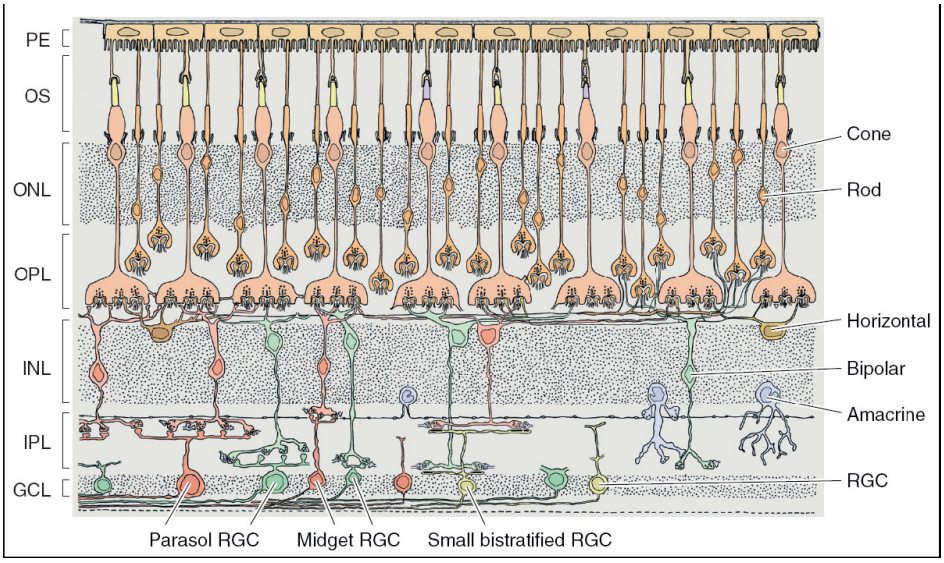

Fig.2 Structure of retina. Retina is a highly organized structure in separate layers containing cell bodies, axons and synapses. Among different cell types of retina, the only cell type that is firing action potentials is retinal ganglion cells. These cells encode the visual stimulation and represent the final output of retina toward next stages in visual system.

The direct path is highly specific or compact, in the sense that one receptor or only relatively few feed into a bipolar cell, and only one or relatively few bipolars feed into a ganglion cell. The indirect path is more diffuse, or extended, through wider lateral connections. Despite the fact that retina is very well organized structure, the information within retina is processed in a very complex manner. The main interest of our report is focused on retinal ganglion cells (RGC). Ganglion cells receive the incoming signals and produce spike trains that contain precise temporal and spatial information about the patterns of light initially detected by the photoreceptors. There are numerous

types of ganglion cells, each of which conveys information about a specific feature of an image detected by the photoreceptors. It has been established that the structure, function, and central projections of RGCs are highly correlated.

The receptive field (RF) is defined as the area of visual space within which one can influence the activity of a neuron. The RF is very often used by neurophysiologists to study the function of visually responsive neurons, because it characterizes the transformation between the visual image and neuronal activity. To describe how a neuron processes the visual image, one must characterize its RF in the joint space-time domain. It is also well known that LGN and RGC have similar center-surround receptive fields.

Direction Selectivity in retinal ganglion cells

The mammalian retina contains several different types of ganglion cells, most of which respond to one or more specific features of a visual image, such as contrast, color, or motion. Some ganglion cell types are motion sensitive, meaning they respond to temporal changes in luminance within their receptive fields, corresponding both to images moving across the field of vision as well as to self-motion of the organism.

A subset of motion sensitive cells responds differentially to the directions of stimulus motion. These Direction Selective (DS) ganglion cells show interesting properties, most of which have been subject for extensive research efforts for the last 40 years. Firstly, Barlow and Levick in 1965 deduced that inhibitory inputs to a DS cell make ineffective excitation for movement in the cell's *null* direction, while excitatory inputs are strongly enhanced for movement in the opposite,

preferred direction. Movement in intermediate directions produces intermediate levels of inhibition or excitation which are used to calculate the degree of directional tuning.

Research conducted on rabbit retinas has revealed two different types of DS ganglion cells in the retina – ON OFF DS cells and ON DS cells. ON OFF DS cells show the response to the movement of a stimulus that is lighter or darker than the background field, while ON DS cells are excited only by objects that are lighter than the background. Several other discrepancies between these two cell types' responses construct a particular spike train signature for each of them. ON OFF DS cells respond to high values of stimulus speeds. ON DS cells, in contrast, respond optimally to stimuli moving at slow speeds. Four subtypes of ON OFF DS cells can be classified by the orientation of the preferred direction of the cell, which points to one end either the horizontal or vertical ocular axis.

Each of the four types responds preferentially to objects moving either to the left, right, top, or bottom. The retina is completely covered by the receptive fields of each subtype of ON OFF DS cell. ON DS cells comprise only three distinct subtypes; the preferred directions of each ON DS cell points in one of three directions aligned with a different set of axes.

The ON-OFF and ON cell types send the directional information to different nuclei, the ON-OFF DS cells to the dorsal lateral geniculate nucleus and the superior colliculus whereas the ON DS cells represent the main input to the accessory optic system. The functional properties of cells in the accessory optic system are consistent with their input from ON-DS cells in many species including primates.

However, in general, DSRGCs represent a model system to investigate information processing within the nervous system. As above stated these neurons respond vigorously to the preferred direction of visual stimulus and remain silenced when stimulus is moving in the opposite null

direction. The intermediate responses are used to calculate the index of selectivity for direction of movement (Fig. 3) as described by Taylor and Vaney in 2002, for a rabbit DSRGC:

$$DSi = \frac{\left\| \sum_i \vec{v}_i \right\|}{\sum_i r_i} \qquad \vec{v}_i = r_i \begin{pmatrix} \cos \varphi_i \\ \sin \varphi_i \end{pmatrix}$$

Recorded activity at all of the presented direction of movement allows us to calculate the firing rate of the neuron as response to the stimulus presentation. Neurons with DSi =1 are selective for one single direction while DSi =0 represents non direction selective neurons. For ON OFF DSRGCs DSi is around 0.5 and direction selectivity for ON DSRGCs is somewhat lower around DSi =0.3.

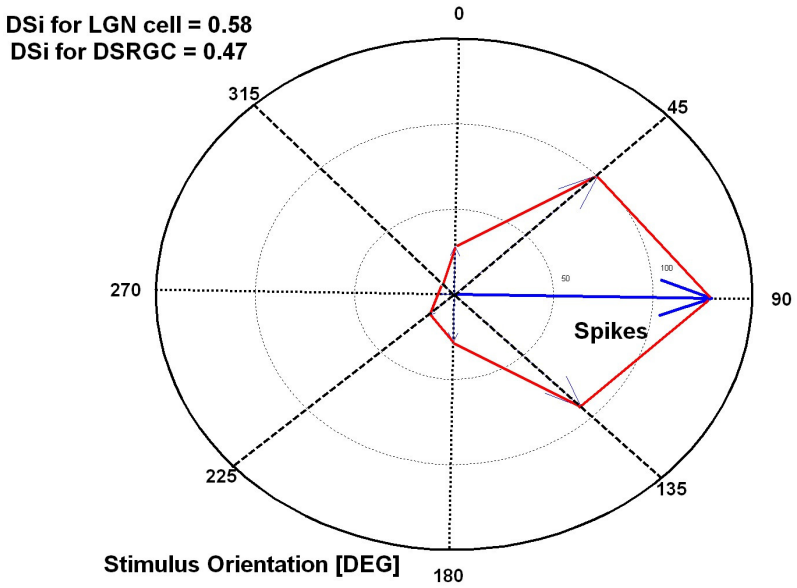

Fig. 3 Direction Selectivity Index calculated from a recorded ON OFF DSRRGC of a rabbit retina, in response to drifting grating bars moving at different directions 45 degrees apart. Preferred direction of this cell is shown to be at 90 degrees with an index of selectivity characteristic for the ON-OFF direction selective cells at this stage in the primary visual cortex, DSi = 0.49.

We show in the followings the neural response of several ON-OFF DSRGCs extracellulary recorded using multi-electrode array and outline some of the basic response properties of this cell type. Firstly, it worth to be noted that ON-OFF DSRGC encode visual information regarding stimulus presented, in a particular manner, by firing boats of rapid activity followed by large periods of silence (Fig.4 & Fig.5). This particular encoding manner is already known as burst-like activity and plays a very important role in information transmission from retina to higher level. Comparing with ON DSRGC, burs-like activity of ON-OFF DSRGC is a spike train signature and can explain some discrepancies between the manners in which direction selectivity is processed at the output of this different retinal ganglion cell types. For example, sharpening in direction selectivity at the output of ON-OFF DSRGCs is more pronounced and simply achieved only by monosynaptic mechanism. For this type of cell we will show that one to one connection from retina to dLGN suffice to have a better signaling of direction of stimulus motion already at LGN level. It is not yet fully understood how exactly the sharpening in direction selectivity at the output of retina is achieved but we will show that burst-like activity in ON-OFF DSRGCs is crucial to sharpens the tuning curves of directional selective responses. RGCs fire remarkably precise (better than a neural response characterized by Poisson statistics), starting with rapid firing at the beginning of an appropriate stimulus presentation followed by a period of silence and ending with another burst at the end of stimulus presentation (Fig.4 & Fig.5). Tuning curves encoding directional selectivity of ON-OFF DSRGCs present a sharp orientation at preferred direction (Fig. 4) based on a fundamental characteristic of neural response of this cell type, namely their enhanced response at preferred direction and weak at intermediate non-preferred direction. However, it is not simply the firing rate which can entirely encode direction selectivity at this level. We built artificial spike trains mimicking ON-OFF DSRGCs with the same indexes of selectivity, firing rate

and directional tuning, following a Poisson distribution. These artificial spike trains did not produce the same degree of directional tuning at the output of their post-synaptic counterpart. If firing rate was the key in a better signaling stimulus direction of motion then we should find the same sharpening in direction selectivity in both cases, recorded ON-OFF DSRGCs and artificial spike trains which mimic them. The only difference between recorded and artificial spike trains was burst-like activity. We found substantially lower burst-like activity in artificial spike trains than in the recorded trains. Additionally, burst rate for artificial trains was not tuned at preferred direction, as was the case for recorded trains, and moreover bursts tuning of recorded trains, were more sharpened, showing an index of selectivity always higher than the index of selectivity of firing rate. We will show in the next chapter how burst-like activity helps in a primordial manner to achieve a better signaling the direction of stimulus motion at the postsynaptic counterpart.

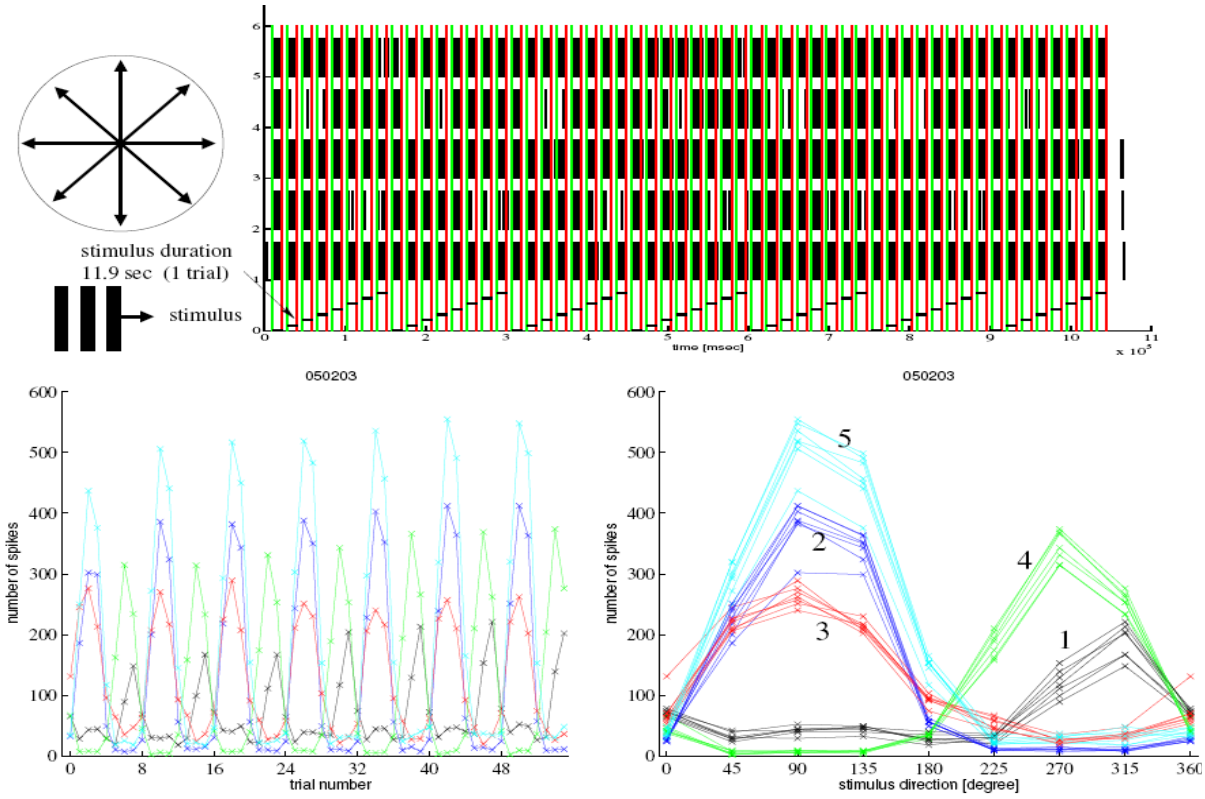

Fig. 4 Neural response extracellularly recorded of five ON-OFF DSRGCs. Stimulus presented consisted in drifting grating bars moved in 7 different directions 45 degrees apart. Direction selective neuron responses were recorded and tuning curves for all trials were built. Three of the cells have preferred direction at 90 degrees and two of them at 270 degrees and 315 degrees, respectively. Left lower side shows the neural response recorded for each trial and right side shows the tuning curves indicating the preferred directions.

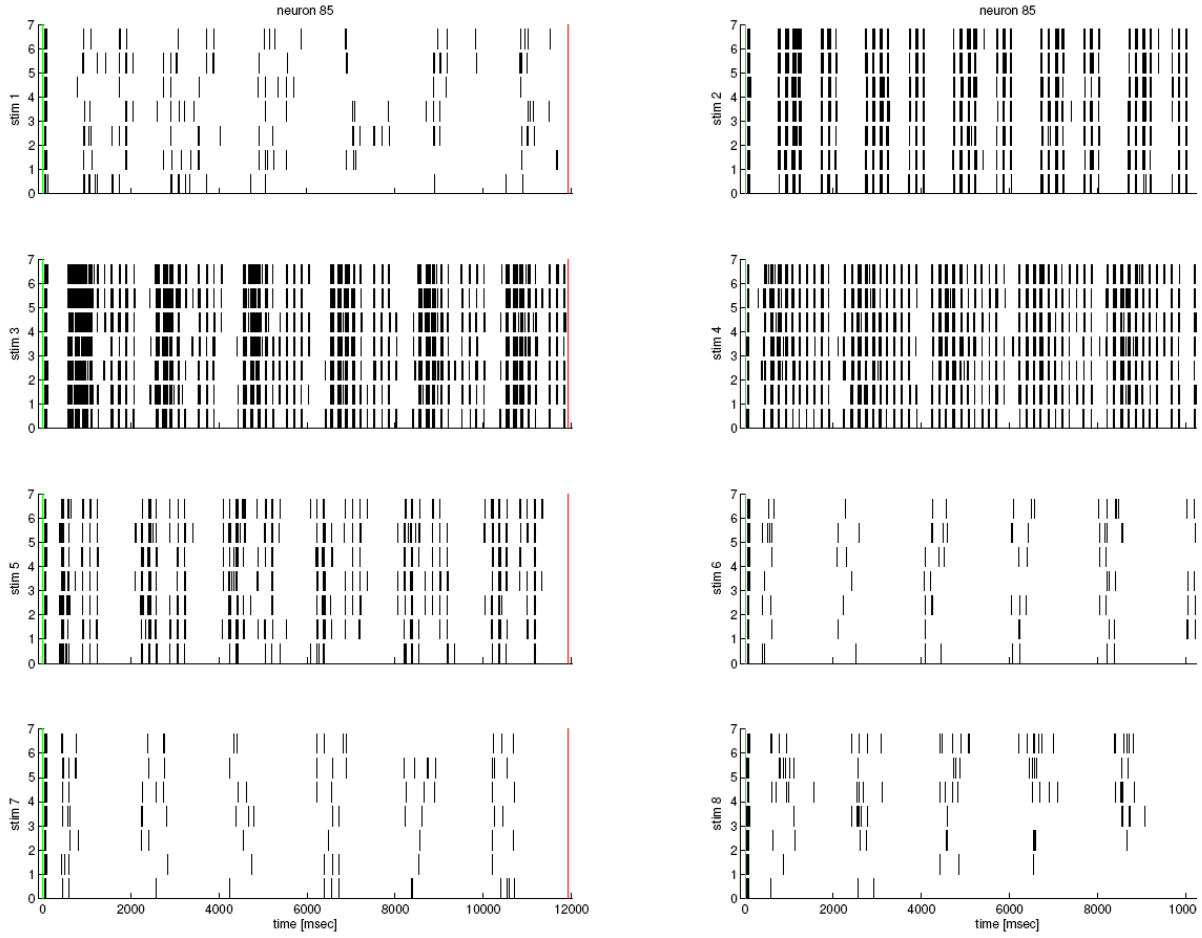

Fig. 5 Recorded activity of an ON-OFF DSRGC with preferred direction at 90 degrees. There are eight raster plots showing the activity of the cell in response to stimulus presentation at eight different directions 45 degrees apart. At trial three (90 degrees), left side second raster plot, we can see that the recorded activity was more intense than at the intermediate response (other raster plots).

Barlow and Levick in 1965 characterized ON-OFF direction selective ganglion cells in the rabbit retina and firstly proposed a model for direction selectivity in which asymmetry of either excitation or inhibition is required. After many research efforts on this topic there is not yet well known exactly where and how direction selectivity in ON-OFF DSRGCs is achieved. Over the years it has been generally accepted that direction selectivity is mediated mainly by the suppression of excitation during movement in the null direction, but not in the preferred direction. Recent results show that excitation and inhibition are already direction selective, that is, excitation is larger during the preferred direction while inhibition is larger during the null direction. This implies that direction selectivity is already computed presynaptically to DSRGCs. However, evidences of postsynaptic computation of direction selectivity where also revealed consisting mainly in postsynaptic interaction of the excitation with spatially offset inhibition. Presumably pre- and postsynaptic mechanisms, at multiple layers and sophisticated connectivity, both determine direction selectivity at DSRGCs (Stasheff and Masland, 2002, Amthor and Grzywacz, 1993, Fried et al., 2002, Taylor and Vaney, 2002).

Sharpening in direction selectivity at retinogeniculate synapse

In a seminal work Levick 1969, demonstrated that neurons postsynaptic to DSRGCs are signaling direction of visual stimulus motion more selectively than their counterparts. He found direction selective neurons in LGN of rabbit to be more directional selective.

Levick model proposed a sharpening in directional selectivity at LGN neuron based on convergent input of different DSRGCs, with similar receptive field but with opposite preferred direction, upon the same LGN neuron (Fig. 6). Blitz and Regehr have shown that most of the LGN cells are receiving inputs from one up to three RGCs. However, it is generally agreed that there is one

single RGC that mainly drives one LGN neuron counterpart (Cleland et al. 1971, Kaplan et al. 1987, Usrey et al. 1998, Sinchich et al. 2007), one third of LGN neurons could receive also inhibitory inputs from the same RGC counterpart but with 1ms delay (so called locked inhibition) and two thirds which could receive inhibitory inputs with different time delay from different RGCs (non-locked inhibition)(Regehr 2005).

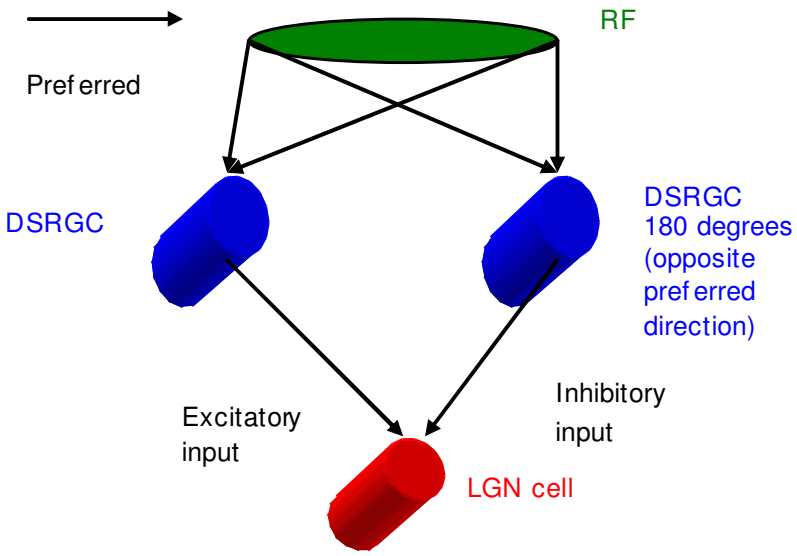

Fig. 6 Levick model for sharpening in direction selectivity at LGN level. Two ON-OFF DSRGCs with similar receptive field (green) but with opposite preferred directions, send convergent excitatory and inhibitory synaptic inputs to the same postsynaptic LGN cell. Inhibitory synaptic input can arrive via a local interneuron or directly to the LGN cell. The mechanism suggest that at non-preferred directions inhibitory input act upon excitatory input and sharpens the degree os direction selectivity.

Recently Casti et al. 2007, and Carandini et al. 2007 have shown that using simple models one could investigate retinogeniculate synaptic mechanism based on the idea that most important fact that influence information transmission from RGCs to LGN neurons could be post synaptic summation and that presynaptic plasticity might not be a primordial mechanism in the editing of retinal spikes

Paired spikes efficacy enhancement was already shown at retinogeniculate synapse. Sequences of rapid firing activity have a better chance to induce postsynaptic spikes than isolated input spikes (Carandini 2007). While single EPSPs on their own do not reach threshold, rapid spiking activity in the DSRGC can trigger LGN spikes (Fig2). It is not yet well understood the role of synaptic plasticity at retinogeniculate synapse, additionally inputs other than retinal afferents (cortical, reticular or brainstem) can complicate modeling LGN neuron discharge. In a simple approach, taking into account only direct synaptic connection between DSRGCs and their postsynaptic counterparts we show, further on in this work, that sharpening in direction selectivity at postsynaptic level is achieved based on intrinsic properties of ON-OFF DSRGCs combined with postsynaptic summation and spike threshold (Fig. 7).

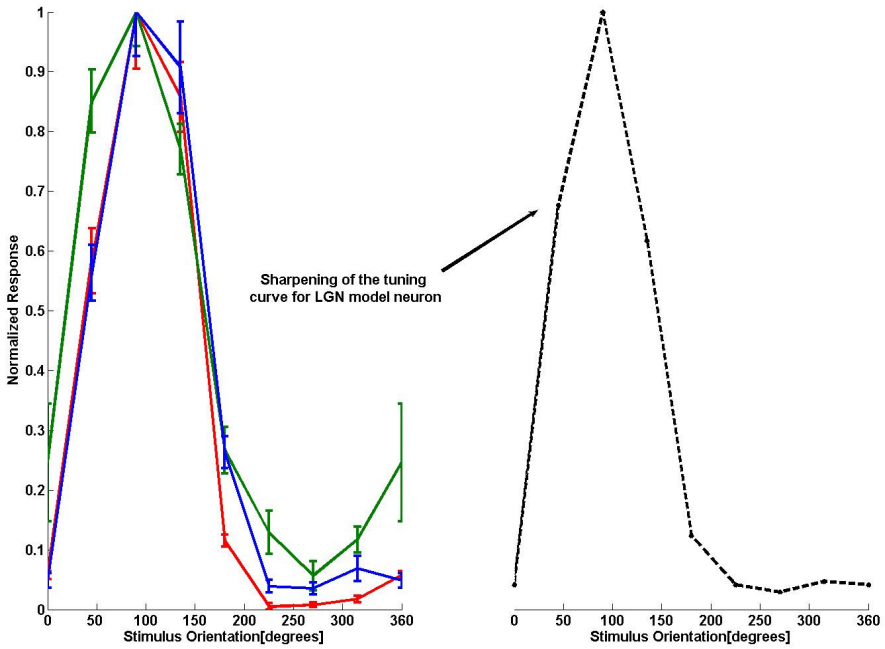

Fig.7 Sharpening of directional selectivity from retinal direction selective ganglion cells to postsynaptic model neurons. (Left) Mean tuning curves of three ON/OFF DSRGC (with preferred direction at 90 degrees of stimulus orientation) recorded in the same retinal patch. Normalized response of the cells is on the Y axis and stimulus orientation on X axis. (Right) LGN model neuron, calculated using the response of excitatory input from DSRGC, shows a sharpening in the tuning curve suggesting a higher degree of directional selectivity.

We have seen up to now how direction selective retinal ganglion cells respond to a stimulus presentation, how their response is encoded in their firing rates tuned at preferred direction and how these neuronal responses characterized by an index of selectivity (Fig.3), can show us accurately the direction of stimulus motion. We also have seen from the neural response (Fig.5) that ON-OFF DSRGCs present a very important characteristic well known as burst-like activity, consisting in rapid boats of firing activity followed by periods of silence (Fig.4). We next will suggest a mechanistic model which help us explain how neurons postsynaptic to ON-OFF DSRGCs are signaling better the direction of stimulus movement.

3. Sharpening in direction selectivity at the output of retina

The estimation of motion direction from time varying retinal images is a fundamental task of visual systems. Neurons that selectively respond to directional visual motion are found in all species. In many of them already in the retina direction selective neurons signal their preferred direction of movement. Recent evidence suggests that direction selectivity is carried from the retina to higher brain areas. Here we adopt a simple model – inspired by recent work of Casti et al. (2008) and Carandini et al. (2007) - to investigate how directional selectivity changes for cells postsynaptic to retinal neurons. Our model analysis shows that directional selectivity increases over a wide parameter range. The degree of directional selectivity positively correlates with the probability of burst-like firing of presynaptic direction selective retinal ganglion cells Sharpening does not increase for polysynaptic inputs. We therefore suggest that sharpening is a simple effect of the intrinsic spiking pattern of the DSRGCs combined with summation of excitatory postsynaptic potentials (EPSP) and spike threshold in postsynaptic neurons.

Background

As early as in the mammalian retina the direction of visual motion is computed by so-called direction selective ganglion cells (DSRGC). These cells signal object movement in a preferred direction and are silent to movement in the opposite, null direction. The cells, however, show an intermediate response to intermediate directions that is used to calculate a characteristic tuning index.

DSRGCs have been extensively characterized in the rabbit retina (Barlow and Levick 1964; Euler 2002; Vaney 1981, 1981b, 1994) but occur in many other species as well (mouse: Weng et al. (2005, Meister&Sanes 2008, Barres&Feller 2009); cat: Stanford and Sherman (1984); rat: Dann and Buhl (1987)).

Retinal direction selective cells can be separated in ON-OFF cells - if they respond at the beginning and the end of an incremental or decremental light stimulus - and in ON cells – if they respond at the beginning of an incremental light stimulus only. In the mouse retina a new OFF direction slective type has been recently discovered (Meister&Sanes, 2008) The ON-OFF and ON cell types send the directional information to different nuclei, the ON-OFF DS cells to the dorsal lateral geniculate nucleus and the superior colliculus (Cleland and Levick 1974a, Vaney et al. 1981a); whereas the ON DS cells represent the main input to the accessory optic system (Buhl and Peichl 1986). The functional properties of cells in the accessory optic system are consistent with their input from ON-DS cells in many species including primates. [in the cat: Grasse et al. (1984); rat: van der Togt et al. (1993); and in primates: Mustari and Fuchs (1989), Hoffmann and Distler (1989).]

One caveat in studying directional selectivity in higher brain areas is the accessibility of these cells. Only occasional responses were recorded in the dLGN of the rabbit. A classical study for

ON-OFF direction selective neurons in the rabbit's dorsal geniculate nucleus (Levick et al., 1969) reports a higher directional selectivity for LGN neurons compared to retinal DSRGCs. On the opposite, direction of motion can be estimated from the population response of many ganglion cells in the retina using multielectrode arrays (Devries et al 1997).

In this study we took advantage of simultaneously recorded DSRGCs and asked under what conditions neurons postsynaptic to the DSRGC provide a more accurate directional tuning. We investigated monosynaptic connections where the recorded spike train of DSRGC provides the presynaptic input to a postsynaptic model neuron. We also checked if polysynaptic inputs from DSRGCs tuned to the same preferred direction led to a further increase of the directional tuning. We adopted a simple integrate-and-fire model that has been validated recently for the retina-geniculate pathway of the cat and primate respectively (Casti et al., 2008; Carandini et al., 2007). The simulated postsynaptic neuron (SPN) receives excitatory input and, in some simulations, inhibitory input from its retinal presynaptic partner. We show that sharpening of directional tuning occurs over a wide range of biophysically reasonable parameters for ON-OFF direction selective cells but less so for ON direction selective cells. To explain the discrepancy we characterize the spike train properties of the two cell types. We find that burst-like activity in one cell type (ON-OFF DSRGC) is responsible for the broad parameter range that lead to directional sharpening. In a last set of simulations we investigate model neurons that receive polysynaptic direction selective inputs. Presynaptic ON-OFF DS cells synapsing onto the same postsynaptic cells do not improve the tuning compared to monosynaptic cells. However, the parameter range describing the strength of presynaptic excitatory input, shifted toward lower values, in order to achieve sharpening in directional tuning at postsynaptic model neuron. In this situation the strength of excitatory synapse does not necessary have to be high in order to achieve sharpening in direction selectivity. By

contrary if two strong excitatory inputs arrive simultaneous at the same postsynaptic neuron, almost each EPSP will give rise to an action potential (AP) at the postsynaptic neuron and no sharpening in direction selectivity can be achieved.

In an important work, in 1988, Soodak and Simpson have shown that neurons in AOS nuclei (of rabbit) have similar basic visual response properties with those of ON DSRGCs which provide direct synaptic input to them. In our simulations we asked whether convergent presynaptic inputs from synchronous ON DSRGCs could sharpen direction selectivity at a postsynaptic cell resembling an AOS neuron. Our results show improved direction selectivity at SPN even if only two ON DSRGCs were combined and suggest that higher sharpening might be achieved if a larger number of ON DSRGCs converge on the same AOS neuron.

Methods

Experimental Data

We used data recorded from retinal ganglion cells of the adult isolated rabbit retina. The data acquisition using a 60 channel multi-electrode array (Multichannelsystems, Reutlingen, Germany) and off-line analysis has been described in (Zeck and Masland, 2007).

Direction selectivity was tested using a square wave spatial grating moved in $N = 8$ equally separated directions $\varphi_i = i \cdot \frac{2\pi}{N}$, $i = 0,1,\ldots,N\text{-}1$. For each direction the grating (spatial frequency 1 cycles/mm) was presented for 7 seconds at a temporal frequency of 1 Hz followed by a stimulus free interval of the same length. The total stimulus length ranged from 600 to 1200 seconds. The spatial extent of the moving grating was ~ 7 μm^2 on the retina. Thus multiple cells were stimulated and recorded simultaneously. Individual tuning curves were obtained considering the firing rate of each cell for each of the eight equidistant directions. Data from 10 ON-OFF DSRGCs and from 3 ON DSRGCs were used in this study.

Direction Selectivity Index

To quantify the directional tuning of a neuron, we used the direction selectivity index (*DSi*) as described by Taylor and Vaney (2002),

$$DSi = \frac{\left\| \sum_i \vec{v}_i \right\|}{\sum_i r_i} \quad , \quad \vec{v}_i = r_i \begin{pmatrix} \cos\varphi_i \\ \sin\varphi_i \end{pmatrix}. \qquad (1)$$

$\vec{v}_i$ is a vector pointing in the direction of the stimulus with the length equal to the number of spikes recorded during presentation of the stimulus (r_i). The *DSi* explains the directional tuning based on the firing rates for different particular movement directions of the visual stimulus. The minimum

value of 0 characterizes a non-directional neuron whereas the maximum value of 1 characterizes a neuron that responds for a single direction of movement. The higher the *DSi* the higher direction selectivity is.

Measure of burst-like activity

In order to have a better understanding of the mechanism that presumably underlies the sharpening in direction selectivity of DSRGCs, we evaluated the burst-like firing of DSRGCs and postsynaptic model neurons. Burst-like firing events were defined as (at least two) spikes occurring after a prolonged period of silence, i.e. inter spike interval (ISI) larger than 50 ms, followed by an ISI shorter than 5 ms (Godwin et al. 1996b; Guido et al. 1995; Lu et al. 1992). Burst rate was defined as the number of burst-like firing events per time. Thus, we scanned the spike train of each cell (10 ON-OFF DSRGC and 3 ON DSRGC) for each stimulus direction (8 different directions) and each stimulus repetition (7 stimulus repetitions at each direction). The burst rate was then quantified as total number of calculated bursts divided by total duration of stimulus presentation for each cell.

Modeling postsynaptic neurons

For modeling neurons postsynaptic to DSRGCs, we used a conductance-based "integrate and fire" (I&F) neuron model that had originally been introduced by Wörgötter and Koch (1991). This model was also used by Casti et al. (2008) to describe the response of LGN neurons to input from retinal ganglion cells (RGCs). The membrane potential $V(t)$ of the I&F neuron is governed by

$$C_m \frac{dV}{dt} = -(V - V_{\text{rest}}) g_m - (V - E_a) \sum_f g_a(t - t_f) - (V - E_e) \sum_s g_e(t - t_s). \qquad (2)$$

An action potential is generated whenever the membrane reaches the threshold V_{thresh} (Fig 1). The first term on the right side of Eq. (2) describes the leakage current while the second term describes the effect of afterhyperpolarization (AHP) following each action potential. The input of the neuron is provided through excitatory channels (third term on right side) resulting in EPSPs. In a single case, we also considered "locked inhibition", i.e. inhibition that follows excitation with a fixed delay Δt_{ie} (Fig3b), and an additional inhibitory current $-(V-E_i)\sum_s g_i(t-t_s-\Delta t_{ie})$ was added. The time-dependent conductances are modeled using "alpha-functions" (Rall, 1967; Jack et al., 1975).

$$g_X(t)=\begin{cases} g_{\max,X}\dfrac{t}{\tau_X}e^{1-\frac{t}{\tau_X}},\ t\geq 0 \\ 0,\ t<0 \end{cases}, \qquad X\in\{a,e,i\}. \qquad (3)$$

We also introduce the membrane time constant given by

$$\tau_m = g_m^{-1}C_m\ . \qquad (4)$$

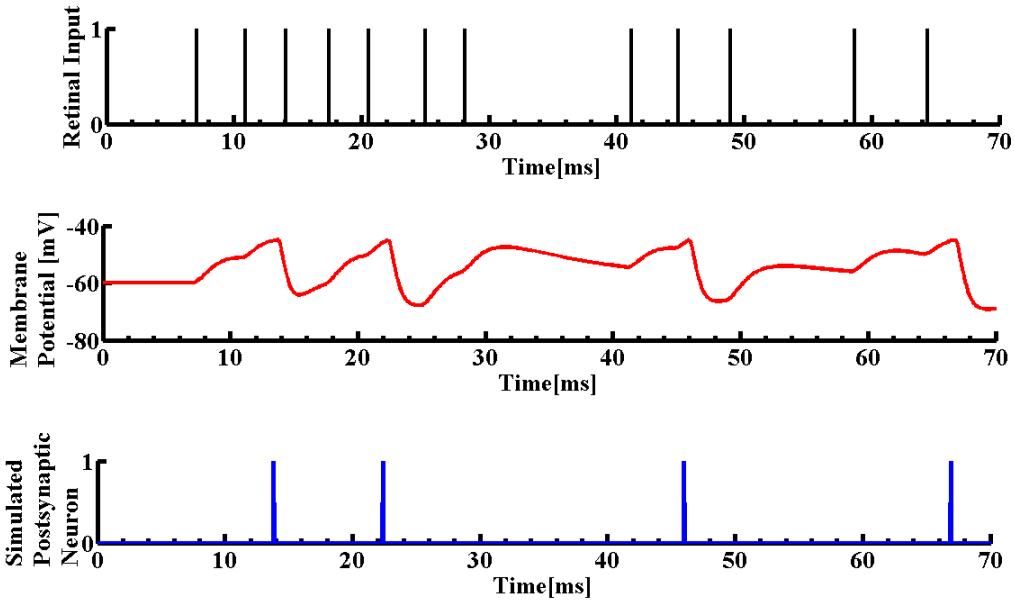

Fig. 1: Simulation of a neuron postsynaptic to direction selective retinal ganglion cell(Transfer ratio for this data segment is aprox. 0.3). a) Spike sequence of a retinal direction selective ganglion cell. The input spikes that provide (excitatory) input to a simulated postsynaptic neuron. b) Time course of the membrane potential V_m of a PMN/SPSN computed by integration of Eq. (2). c) Spike sequence of the SPN. Resulting firing events of the SPN (firing threshold is V_{thresh} = -45mV).

Table 1 summarizes the values used for the different model parameters. In the majority of plots, we varied the maximum excitatory conductance (while other parameters were kept constant). We set all parameters that were kept constant, to values found by Casti et al. (2008) to best describe the behavior of LGN neurons. Equation (2) was integrated using a first order Euler method with a time step of 0.1 ms.

Table 1: Parameter values used in this study (for parameter that can have different values, its typical value is highlighted in bold face). The membrane conductance can be calculated from Eq. (4), $g_m = \tau_m^{-1} C_m$.

Parameter	Value(s)
Membrane time constant τ_m	5 / 8 / **10** / 12 / 15 / 20 ms
Membrane capacitance C_m	1 nF
(Membrane conductance g_m	0.2 / 0.125 / **0.1** / 0.07 / 0.05 µS)
Resting potential V_{rest}	-60 mV
Threshold potential V_{thresh}	-45 mV
Excitatory reversal potential E_e	20 mV
Inhibitory reversal potential E_i	-90 mV
Afterhypolarisation reversal potential E_a	-95 mV
Maximum excitatory conductance $g_{\text{max},e}$	0.02 / 0.03 / 0.04/0.05 / 0.06/0.07 / 0.1 / 0.15 µS
Maximum inhibitory conductance $g_{\text{max},i}$	**0** / 0.02 / 0.03 / 0.04 / 0.06 / 0.1 / 0.15 µS
Maximum afterhypolarisation conductance $g_{\text{max,a}}$	0.59 µS
Excitatory time constant τ_e	1 ms
Excitatory time constant τ_i	1 ms
Afterhypolarisation time constant τ_a	0.5 ms
Time delay for locked inhibition Δt_{ie}	1 ms

Index of Sharpening

To compare the direction selectivity of the output of the simulated postsynaptic neuron (SPN) with that of the driving neuron, we define the index of sharpening as

$$iS = \frac{DSi(SPN)}{DSi(DSRGC)}. \quad (5)$$

$iS > 1$ means that the SPN shows higher directional selectivity than the presynaptic neuron.
In order to investigate the role of presynaptic property (i.e. burst-like activity) we calculated index of directional selectivity from burst rate in the same manner as from firing rate in response to stimulus presented at 8 different directions of movement. For particular values of gmaxe (see Table2) at which the postsynaptic DSi is highest we found DSi burst rate closely matching DSi SPN. Thus :

DSi(SPN) ≈ DSi(Burst) . Further on the linear approximation:

$$iS \approx \frac{DSi(Burst)}{DSi(DSRGC)} \quad (5.1)$$

Spike Transfer Ratio

Similar to Casti et al. (2008), we define the spike transfer ratio,

$$TFR = \frac{\#\text{SPN spikes}}{\#\text{DSRGC spikes}}, \quad (6)$$

where "#" stands for "number of" (or "rate of"). According to Casti et al. (2008), the *TFR* of LGN-cells for input from (non-direction selective) RGCs is between 0.07 and 0.7 (with median 0.34, see table 2 in Casti et al., 2008).

In our simulations the *TFR* usually depends on stimulus direction φ_i and thus *DSi* and *iS* are often calculated from simulation runs with different *TFR*. For this reason, we use the maximum *TFR* value over all stimulus directions,

$$TFR = \max_i TFR(\varphi_i) \quad . \qquad (7)$$

In the figures of the result section we highlight those results where *TFR* is within the range [0.07, 0.7].

Artificial spike trains

In order to investigate which properties of spike trains effect sharpening, we also generated "artificial spike trains". These spike trains have the same average spike rates for different stimulus directions - and thus the same *DSi* - as spike trains recorded from DSRGCs. The firing probability was equally distributed over time according to a Poisson process except for defined refractory periods after each spike event. Spike trains with refractory period of 2 ms, 5 ms and 10 ms were generated.

Results

Sharpening of direction selectivity from ON-OFF direction selective cells

The model adopted here incorporates several mechanisms that presumably dictate the editing manner of presynaptic input - the membrane passive properties of the simulated postsynaptic model neuron (SPN), (i.e. the membrane time constant), the excitatory synaptic conductance that determines the EPSPs and inhibitory synaptic conductance to characterize IPSPs.

We firstly looked at the directional tuning of the SPN response that receive monosynaptic input according to the spike timing of direction selective retinal ganglion cells (DSRGCs) recorded extracellularly with a multi-electrode array. While only the strength of synaptic excitatory conductance (parameter gmaxe) was varied, the other parameters were kept fixed as in Table1 (similar biological plausible values as proposed by Woergoetter and Koch, 2001, and Casti 2008). We found that the direction selectivity index DSi, Eq. (1), of the SPN was higher than that of the presynaptic ON-OFF DSRGC over a considerable range of the excitatory synaptic conductance (Fig 2a). The strength of the synaptic conductance was varied under the assumptions that the ratio of pre- and postsynaptic cells firing rate is restricted to the interval 0.07 and 0.7 (Casti 2008) and took values from 0 to 0.12 uS. The degree of sharpening – the index of sharpening (iS)- is expressed in the following as the ratio of post- and presynaptic direction selective indices. (Eq.5). The main reason for sharpening is the relative spike reduction in response to non-preferred stimulus directions. Fig 2a shows an example of one ON-OFF DSRGC and its SPN counterpart with directional tuning for different gmaxe values. DSi for this retinal cell was 0.49 and preferred direction at 90 degrees. With excitatory synaptic input only, the SPN counterpart in this example, is more directional selective than its retinal driver. We found iS for SPN higher than 1 for gmaxe = 0.06 uS (iS=1.4) up to gmaxe=0.1(iS=1.2).

We calculated the degree of sharpening for a total of ten ON-OFF direction selective neurons (Fig 2b) up to a value of gmaxe that leads to a transfer ratio of 0.7. For all simulated cells we obtain sharpening of directional selectivity.

However, weak synaptic inputs (i.e. gmaxe < 0.04 μS) did not lead to sharpening in direction selectivity, except for only one of the cells, mainly due to a very low transfer ratio (TFR, Eq.7) (i.e. bellow 0.07 minimum limit) and thus iS=0. As the strength of excitatory synaptic input grew, for 8 (out of ten) cells iS stepped over 1 already at gmaxe=0.04 μS (Fig 2b), for two cells TFR still remained under the limit value, and thus iS was set to 0. Excitatory synaptic inputs with gmaxe ≥0.05 μS always led to iS>1. Mean value (Fig 2b-red curve) of iS =1.30 (std=0.20, n=10) at gmaxe=0.05 μS and has slightly decreased to iS=1.11 (std=0.06, n=10) at gmaxe=0.1 μS. For a strong synapse as described by gmaxe=0.12 μS, iS =0 again, while TFR exceeds maximum value of 0.7. At this value already almost every EPSP is capable to provoke an AP at the SPN and thus DSi of the SPN approximate DSi of presynaptic cell, situation depicted by green rectangle area in Fig. 2b which shows that iS stays close to 1 if TFR was ignored. Mean iS (at gmaxe=0.12 μS without taking into consideration TFR) = 0.97(std= 0.02, n=10).

The degree of sharpening however depends on the tuning of the presynaptic cell. For an excitatory synapse of gmaxe = 0.06 μS, the iS decreases for increasing direction selective indices of retinal drive as indicated in Fig 2c. As expected, for ON-OFF DSRGCs with low DSi, sharpening at the SPN counterpart is stronger than that observed for high presynaptic DSi, while maximum possible value of DSi is 1(a cell selective for only one direction of stimulus movement) highly selective ON-OFF DSRGCs do not lead to much more directional selective postsynaptic counterparts. Fig2d shows inverse proportionality between indexes of sharpening (iS) at SPN and DSi at retinal cells. iS is decreasing when DSi is increasing.(iS decreases with a slope as calculated from Fig 2d

Tan(α)=diff(iS)/diff(DSi); α= 67.72°). In conclusion sharpening in directional selectivity was achieved for all tested ON-OFF DSRGCs and was more prominent for presynaptic inputs with a lower DSi.

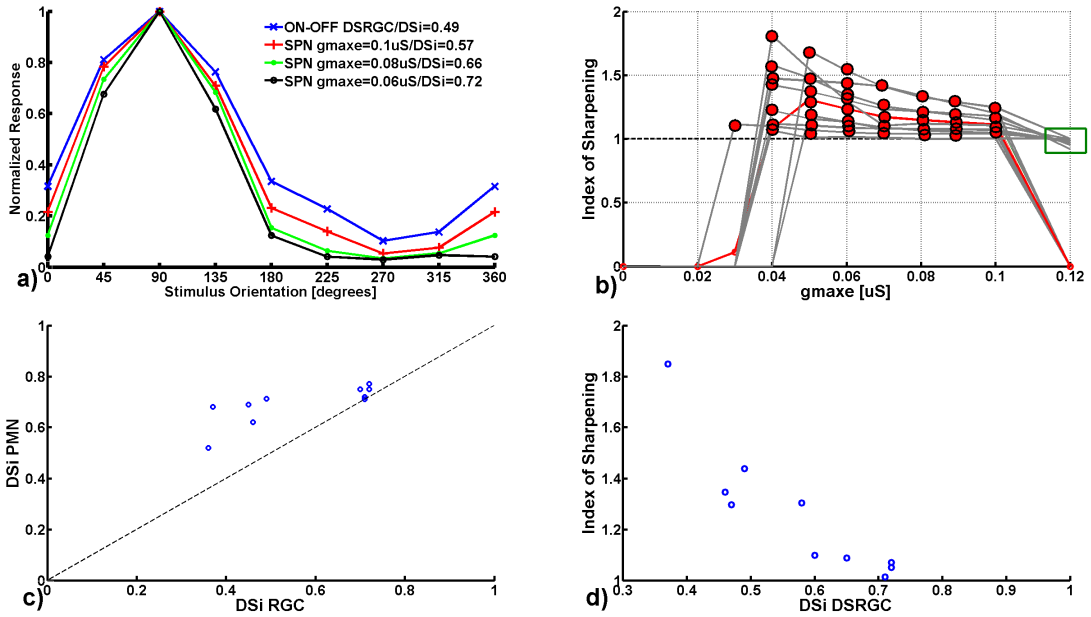

Fig.2: The directional tuning of model neurons increases if ON-OFF direction selective cells provide monosynaptic input. Index of Sharpening iS = DSi(PMN)/DSi(DSRGC), Eq. (5). Red dots indicate the values for which transfer ratio was between the considered limits of 0.07-0.7.

a) Normalized (mean) responses (averaged over 7 trials of 12sec each) of an ON-OFF (blue curve) and of SPNs receiving excitatory input from the DSRGC for different synaptic conductances $g_{max,e}$. While the DSRGC has direction selectivity index DSi = 0.49, the simulated neurons have higher DSi values and thus iS > 1: For $g_{max,e}$ = 0.1 µS (red curve) we have DSi=0.59 resulting in iS = 1.2. For $g_{max,e}$ = 0.08 µS (green curve), we have DSi = 0.66 and iS = 1.34, for $g_{max,e}$ = 0.06 µS (black curve) DSi = 0.71 and iS = 1.4

b) Index of sharpening (IS) computed from 10 ON-OFF DSRGCs and their simulated postsynaptic counterparts for different maximum excitatory conductance $g_{max,e}$ (black curves). On the average (red curve), we find sharpening (IS > 1) for $g_{max,e} \geq 0.04$ µS up to 0.1 µS. For $g_{max,e} \geq 0.12$ µS no significant sharpening is observed (DSi(PMN) ≈

DSi(DSRGC), iS ≈ 1) because each input spikes triggers an output spikes in the simulated postsynaptic neuron for high synaptic conductances, see green rectangle. For DSRGCs with high DSi, maximum iS=DSi(PMN)/DSi(DSRGC) is usually lower than for DSRGCs with low DSi.

c) Direction selectivity index for postsynaptic model neuron is higher than direction selectivity index of ON-OFF DSRGCs (for all cells). For this figure gmaxe= 0.06 µS.

d) The degree of sharpening depends on presynaptic direction selectivity. The higher the DSi of presynaptic cell the lower the iS at SPN.

In a next set of simulations we investigate how robust sharpening is against variations (of postsynaptic parameters) in the membrane time constant (Fig 3a) and against introduction of additional inhibitory conductance (Fig 3b).

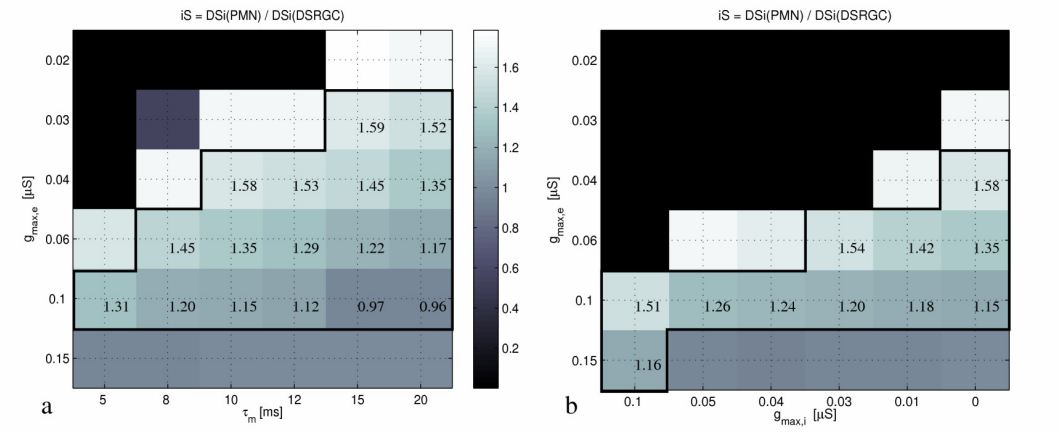

Fig. 3: Index of sharpening for a postsynaptic model neuron that receives input from a DSRGC (050414_ch78) in dependence on maximum excitatory conductance $g_{max,e}$ and membrane time constant τ_m **a)** or maximum inhibitory conductance $g_{max,i}$

b) The black contour line highlights areas where TFR is within the range [0.07, 0.7].

We varied the membrane time constant in order to capture the additional effect that this postsynaptic parameter could have over the iS. As membrane time constant increases (membrane conductance decreases) we found that sharpening is achieved at low gmaxe values (Fig.3a, for τ_m=15 ms, gmaxe =0.03 μS, iS=1.59). However, if strength of excitatory synaptic input is increased no sharpening is achieved if τ_m >15 ms. (iS=0.97). By contrary, at low τ_m values a sharpening is achieved only for strong excitatory synaptic input (τ_m = 5ms, gmaxe=0.1 μS, iS=1.31). At any fixed τ_m value the degree of sharpening at SPN respects the same trend and decrease as the strength of gmaxe increase.

Thus, at biologically plausible values for time membrane constant we found sharpening in direction selectivity at postsynaptic model neuron for a large interval of gmaxe values (Fig3a). Stimulus that is larger than center of receptive field could provoke additional (excitatory and/or inhibitory) inputs from neighbor retinal cells directly or by mean of local interneurons (Alitto & Usrey 2005, Carandini 2007). To investigate the effect of such a situation additionally to excitatory synaptic input we used inhibitory synaptic input convergent on the same postsynaptic model neuron. For the inhibitory conductance we used a fixed time delay of 1 ms with respect to the excitatory inputs. Both, excitatory and inhibitory synaptic inputs are sent by the same DSRGC main driver. Time locked excitation and inhibition has been found in the retinogeniculate pathway (Regher et al. 2005). Variation of these parameters under the transfer ratio restriction demonstrates that over a wide range of model parameters the postsynaptic neuron has a higher index of direction selectivity.

As expected if gmaxi increased (strong inhibition) gmaxe must also increase in order to achieve sharpening at SPN. Similarly with previous simulations, at any fixed gmaxi value iS decreases with increasing gmaxe (Fig3b).

Altogether, these scenarios presented that far suggest that direct monosynaptic excitatory input suffice to achieve sharpening at postsynaptic neuron for a wide range of biologically plausible synaptic strengths. Additional parameters, describing postsynaptic neuron properties or involving polysynaptic mechanism, do not radically change the sharpening in direction selectivity at SPN.

Sharpening of direction selectivity from ON direction selective cells

In addition to the ON-OFF direction selective neurons, we investigated a second type of direction selective cells – the ON DS cells. These cells have broader directional tuning and thus smaller DS indices than ON-OFF DS cells.

In contrast to the extensive sharpening of small DS indices from ON-OFF cells (Fig 2c) we do not find much sharpening for the three ON DS cells investigated (Fig 4a). The simulations were performed analogous to the ON-OFF DS cells with the constraint on the transfer ratio. For one of the cells we found sharpening at SPN only for a single gmaxe value (Fig4a, gmaxe = 0.1 µS, iS = 1.1) while the other two cells presented iS higher than 1 for a restricted range of gmaxe values (gmaxe $\geq$ 0.07 µS and gmaxe $\leq$ 0.1 µS). The degree of sharpening is less pronounced than in the case of ON-OFF DSRGCs and in mean it starts exceed 1 only at gmaxe=0.07 µS when iS = 1.11. Beyond gmaxe = 0.1 µS no sharpening is achieved due to the fact that such strong synaptic input is generating almost at each EPSP an AP at SPN so that iS tends to be almost 1 (as indicated by the blue curve in Fig4a if TFR were ignored). Thus, for ONDS RGCs we found less sharpening when comparing with ON-OFF DSRGCs in the same simulation conditions.

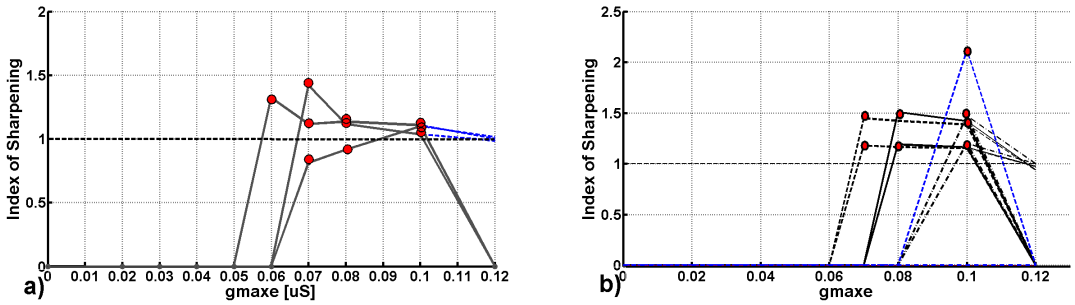

Fig 4. iS for ON DS and Artificial spike trains

a) Index of sharpening for 3 ON DSRGCs . For ON-DSRGCs, sharpening is usually less pronounced and achieved only for higher conductances $g_{max,e} \geq 0.07$ μS. Red dots in the plots indicate gmaxe values for which TFR is in the validation domain, while blue dashed lines indicate the iS value if TFR were ignored.

b) Index of sharpening for artificial spike trains and post-synaptic model counterparts. Refractory periods are 2 ms (dashed curves), 5 ms (continuous curves), and 20 ms (dash-dotted curves).

For each refractory period two set of artificial spike trains were generated that have the same firing rates and thus the same DSi values as two ON-OFF DSRGCs, namely 'DSRGC_ch55 and 'DSRGC_ch78'. Blue plots represent artificial spike trains that mimic an ON DS cell. Best sharpening is obtained for 2 msec refractory period spike trains for ON-OFF DSRGCs and is less present as refractory period increase. At 20 msec iS>1 only at gmaxe = 0.1 μS. For ON DSRGC we found iS>1 only for a single gmaxe value = 0.1 μS.

Sharpening of directional selectivity from artificial spike trains mimicking direction selective neurons.

Apparently the presynaptic degree of directional tuning does not provide evidence how the sharpening works. We therefore considered artificial spike trains that mimicked the firing rate and thus directional tuning of ON-OFF as well as ON DS cells. The spike trains followed a poisson distribution. We calculate the postsynaptic sharpening for a total of nine artificial spike trains. Each spike train mimicked the directional tuning of either an ON-OFF DS cell with high index of selectivity(DSi=0.72), an ON-OFF DS cell with smaller index of selectivity (DSi=0.49) and an ON DS cell(DSi=0.34). For each of the three firing rates we consider three refractory periods: 2msec, 5 msec and 20 msecs. The best sharpening is found for short interspike intervals (i.e. refractory period of 2 msec). This holds true for simulated spike trains with different average firing rate (Fig4b blue and black dashed curves). For this spike trains (with small refractory period of 2 msec) the sharpening at SPN is achieved for an interval of gmaxe =[0.07 – 0.1] μS. Increasing refractory period at 5 msec we found sharpening for a more restricted interval of gmaxe = [0.08 – 0.1] μS (Fig4). For the spike trains with 20 msec refractory period we found sharpening only for gmaxe=0.1 μS. For the artificial spike trains mimicking ON DS cell we could see sharpening only at gmaxe=0.1 μS and only if refractory period was set at 2 msec (Fig4b blue dashed curve). Constructed artificial spike trains have the same firing rates as the retinal recorded cells which they mimic. If firing rates of the presynaptic cell would be responsible for sharpening at postsynaptic neuron, than one would expect similar iS (and for similar gmaxe values) to be obtained at the output of artificial spike trains with the same DSi as the recorded cells.

Burst-like spiking is responsible for sharpening of directional selectivity

Our results presented so far indicate that sharpening of directional tuning does not depend on the neuron's firing rate that is different for the different presentation directions (compare Fig 2b and Fig. 4). Artificial spike trains with poisson statistic suggest that intrinsic spike train properties are responsible for sharpening of directional tuning. We therefore investigated the intrinsic spike train properties of ON-OFF DSRGCs. We selected a parameter often used in the analysis of LGN neurons: the percentage of bursting. Burst-like events are identified and quantified as described in Methods (Section 2.3). We calculated the burst-rate in the response of ON-OFF DS cells as well as ON DS and artificial poisson-like spike trains.

Fig5 a,b,c show the tuning curves for three ON-OFF DSRGCs calculated from firing rate (red curve) and burst rate (blue curve). The preferred direction indicated by maximal firing rate coincides with the preferred direction calculated from burst rate. That is, at preferred direction ON-OFF DSRGCs show burst-like activity more than at intermediate directions. In this way the probability of evoking an AP at SPN becomes higher at preferred direction while two (or more) closed (in time) EPSPs are more successful in rising membrane potential of SPN above the threshold. This phenomenon is known as paired spike enhancement and has been demonstrated at many synapses (Usrey et al. 1998, Carandini et al. 2007). The burst rate for ONDS cells and artificial spike trains was almost equal zero (Fig5d,e). Mean burst rate (the average for all 7 stimulus repetitions) at preferred direction was 0.38 [bursts/sec], for the in Fig5d, and did not exactly matched the preferred direction of 315º indicated by firing rate tuning curve (burst rate tuning curve show a maximum at 0 º). For all three ON DSRGCs we investigated the mean burst rate at preferred directions was 0.29[bursts/sec]. For the ten ON-OFF DSRGCs we found a mean

burst rate at preferred direction (of 9.40 [bursts/sec]) significantly higher than for ON DS cells or artificial spike trains. It is already well known that these two different RGC types posses different spike train signatures (Zeck et al, 2007).

The burst rate for each presentation direction can be used to calculate the degree of directional selectivity. Once we calculated the burst rate at each direction of stimulus presentation we next used DSi (see Methods) in a manner similar to that used for firing rate, and we calculate the direction selectivity index for burst-like spiking.

The directional selectivity calculated from bursts is higher than the directional selectivity obtained from firing rates (Fig 6a). For all of the cells we used in this study calculated DSi from burst rate was higher than DSi presynaptic but very close to DSi postsynaptic calculated from firing rates when excitatory synaptic input has the strength which leads to highest DSi at SPN (Table2). As in the Eq.5, the sharpening index is calculated as the ratio of post and presynaptic indices of selectivity. While postsynaptic DSi's calculated from firing rates match DSi's calculated from bursts at presynaptic cells, consequently the ratio of the two indices (DSi burst and DSi firing rate) closely corresponds to the index of sharpening (Fig6b, linear fit Eq5.1) for all ten ON-OFF DSRGCs at the synaptic maximum conductance which lead to the highest sharpening in direction selectivity. As a consequence, burst-like activity in presynaptic ON-OFF DSRGCs could closely predict the degree of sharpening at postsynaptic target under these circumstances. Fig6b suggest how the strength of sharpening in direction selectivity could be inferred at presynaptic level already. That bursts are recognized to be very efficient in transmitting information at different stages within the brain is already well known. In our example burst-like activity seems to be the key in signaling better the direction of motion of visual stimulus at the output of retina.

Table 2. Parameter values for ten investigated ON-OFF cells. Chxx_xx indicate the identity of the cell and retinal patch. DSi SPN closely matches DSi Burst Rate. Values of gmaxe indicated the synaptic strength at which the DSi SPN is highest.

Cell	DSi Burst Rate	DSi SPN	gmaxe (μS)
Ch 55_050203	0.75	0.75	0.05
Ch 78_050203	0.84	0.80	0.05
Ch 25_050203	0.77	0.77	0.05
Ch 85_050203	0.73	0.73	0.04
Ch 55_050414	0.77	0.73	0.04
Ch 72_050414	0.71	0.68	0.06
Ch 84_050414	0.76	0.80	0.05
Ch16	0.74	0.76	0.05
Ch36	0.71	0.71	0.05
Ch46	0.74	0.78	0.05

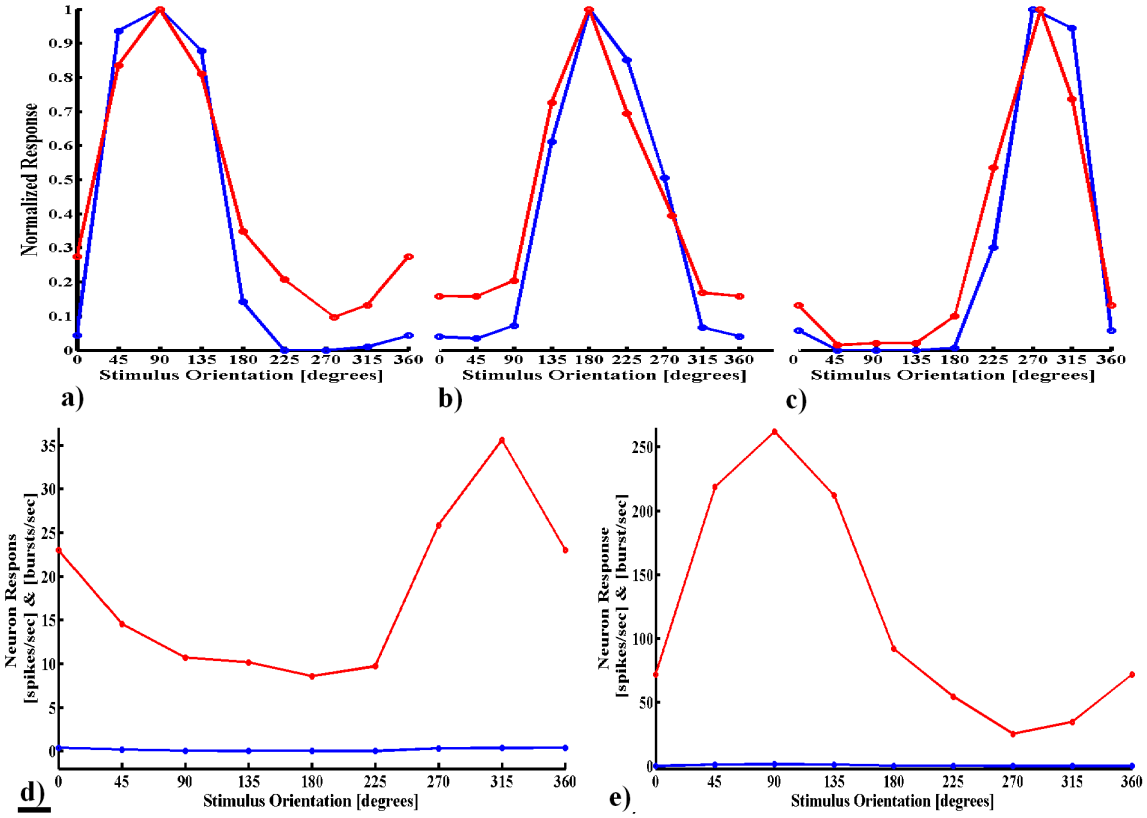

Fig. 5: Normalized firing rates (red curves) and burst rates (blue curves) of three ON-OFF-DSRGCs, DSRGC_ch55 **a)**, DSRGC_ch74 **b)**, DSRGC_ch78 **c)**, of an ON-DSRGC DSRGC_ch17 **d)**, and an artificial spike train with 2ms refractory period that has the same firing rates as DSRGC_ch55 **e)**. For ON DS cell and artificial spike train burst like activity is very low.

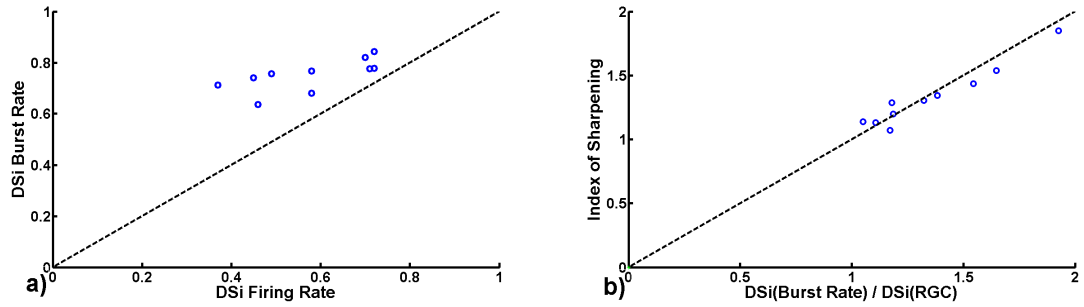

Fig 6. a) Direction selectivity indexes for ten ON-OFF DSRCs. DSi calculated from burst-like activity is always higher than DSi calculated from firing rates in response to stimulus presentation.

b) Index of sharpening accurately matches the ratio of selectivity indexes calculated from burst and firing rates. While burst-like activity is more pronounced at preferred direction, this intrinsic presynaptic property plays a prominent role

in sharpening of direction selectivity at postsynaptic neuron. Index of sharpening is approximated as Eq.5.1 and thus can be predicted by ratio of the two directional selectivity indexes.

Polysynaptic directional selective input onto one model neuron

So far we considered monosynaptic connections of a DSRGC with a model neuron. It is assumed that several retinal cells can converge on the same postsynaptic target (Regehr et al. 2005, Sinchich et al. 2007, Usrey et al. 1998). However, the synaptic strength of each parameter is unknown. In the following we consider polysynaptic input with equal weights from several DSRGC to a model postsynaptic neuron and asked if simultaneous convergent synaptic inputs from ON-OFF DSRGCs with the same preferred direction can lead to a higher sharpening as compared to previously analyzed monosynaptic scenario.

We recorded three ON-OFF DSRGCs in the same retinal portion responding preferentially to the same direction of stimulus movement (90 degrees preferred direction). In a second recording portion we recorded other three pairs, each comprising two neurons with same preferred direction (180, 0 and 135 degrees respectively). In this way we formed in total 6 pairs of combined ON-OFF DSRGCs. We calculated cross correlation histograms (CCH) for these pairs of neurons simultaneously recorded. Further on we aligned the spike trains of formed pairs in order to form simultaneous synaptic inputs to the same postsynaptic neuron. We found a correlated activity with a time lag in CCH of 2 ms for which a maximum correlation between their spike trains was achieved.

In each pair of ON-OFF DSRGCs sending convergent excitatory inputs to the SPN, each cell has different DSi. At the output of model neuron we always found a sharpening in direction selectivity

as compared to any individual DSRGC. However, for the input neuron with the highest DSi the degree of sharpening was lower as compared to the monosynaptic case . For the six pairs of neurons presented in Fig7 a) direction selectivity index at postsynaptic neuron is higher than (DSi SPN = [0.73; 0.74; 0.75; 0.77; 0.79]), presynaptic direction selectivity indices (DSi RGC Є [0.37-0.72]).

Comparing with monosynaptic mechanism, two excitatory synaptic inputs of the same strength (of cells with the same preferred direction) simultaneously converging on the postsynaptic model neuron did not improve the degree of sharpening at the postsynaptic output (Fig 7b). However, the effect of simultaneous polysynaptic input consisted in shifting the range of the values for gmaxe at which sharpening in direction selectivity was produced. This shift was toward lower gmaxe values. As expected, if two simultaneous excitatory synaptic inputs converge on the same postsynaptic target, then the strength of the synaptic conductances must not be too high. At gmaxe=0.03 μS already the maximum sharpening is achieved. When gmaxe is increased, the number of APs at SPN increased also and for gmaxe =0.07 μS the transfer ratio is already exceeding the maximum limit of 0.7.

This result suggest that, even if the synaptic mechanism involve more retinal projection converging on the same postsynaptic target (Regehr et al. 2005, Usrey et al. 1998) only one single cell is mainly driving the postsynaptic counterpart and thus dictating its response properties including the degree of direction selectivity.

Part of the cells recorded on the multielectrode array in our experiments, were proved to be non-directional selective and thus have a very low index of selectivity, bellow 0.1. We further asked what could be the effect of two cells, from the same recording patch, one directional selective and one non-directional selective (NDS) sending convergent excitatory input to the same model

postsynaptic neuron. Thus, we selected two NDS-RGCs from the same recording patch and combined them separately, in pairs of two, with four different ON-OF DSRGCs. For each of the pair formed (one NDS and one ON-OFF DSRGC) we found at the postsynaptic simulated neuron an index of sharpening less than 1. Fig7 c shows the situation as described above. In all of the combinations we found DSi SPN smaller than presynaptic DSi DSRGC meaning that no sharpening in direction selectivity can be achieved in this condition. dLGN in the thalamus is a target for multiple retinal ganglion cell types but the most important is that they that each type apparently terminates on a distinct set of dLGN neurons and that these neurons are often segregated in separate sublaminae or subnuclei of the dLGN (Berson 2008). In our simulations we show that if hypothetically a direction selective and a non-direction selective RGC would project on the same postsynaptic target, the output would loose information regarding direction of stimulus motion.

Taking advantage of multielectrode array technique we further considered polysynaptic excitatory inputs consisting in five ON-OFF DSGRCS (from the same recording patch) driving one postsynaptic model neuron (Fig7 d). We wanted to test if neurons selective for different preferred directions (90, 270 and 315 degrees respectively) lead to sharpening in direction selectivity at the simulated postsynaptic neuron. For ON-OFF cells indices of selectivity were higher than DSi SPN and thus we could not observe a sharpening in directional selectivity at SPN (DSi SPN =0.38 and DSi ON-OFF DSRGCs = 0.41; 0.49; 0.65; 0.72; 0.72). Thus, at least in our simulation conditions, polysynaptic mechanism involving neighboring ON-OFF DSRGCs with the same strength of the excitatory synaptic conductance but with different preferred directions projecting on the same postsynaptic target do not improve the degree of sharpening at postsynaptic level, by contrary the output is signaling less the direction of stimulus movement.

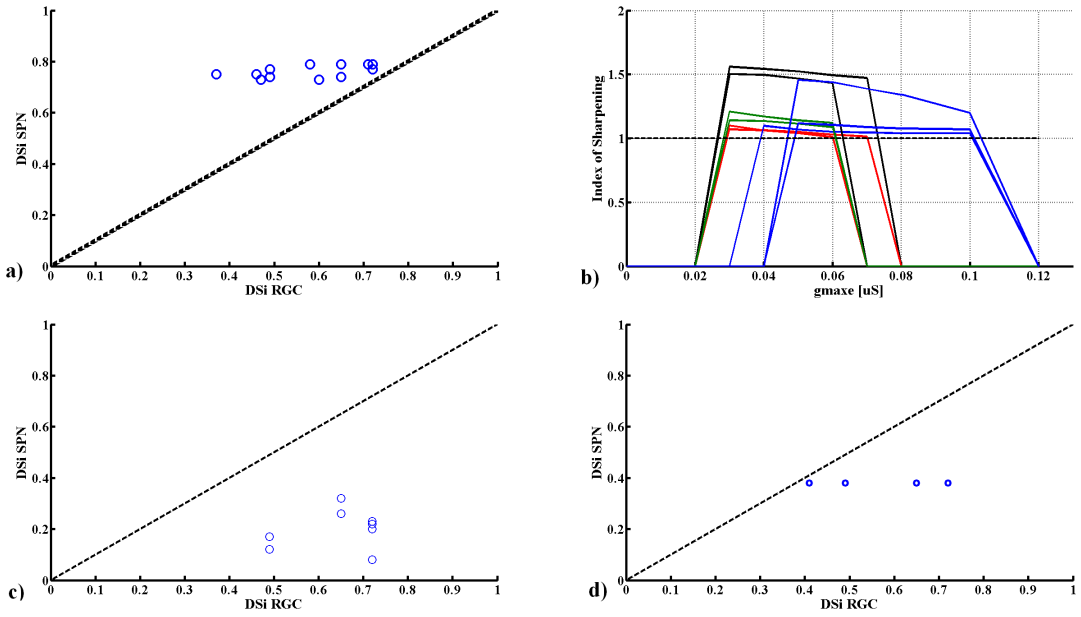

Fig7 a) Sharpening in direction selectivity achieved from polysynaptic inputs formed by pairs of two ON-OFF DSRGCs . SPN shows a higher DSi for each pair. Synaptic strength was set at gmaxe= 0.06 µS.

b) Index of sharpening for three different ON-OFF DSRGCs which send monosynaptic inputs to the postsynaptic cell (blue curves) and index of sharpening for each combination pair of two cells in polysynaptic mechanism(red, green and black curves). The degree of sharpening is almost the same comparing the mono and polysynaptic scenarios. The effect in case of two convergent inputs on the same SPN can be noticed in iS >1 for lower values of gmaxe (i.e. starts at 0.03 µS for polysynaptic case and at 0.04 µS for monosynaptic case). If gmaxe is increased no sharpening is observed already at gmaxe = 0.07 µS for polysynaptic case while for monosynaptic connection iS is still higher than 1 up to gmaxe = 0.1 µS.

c) ON-OFF DSRGC and non-DSRGC synapsing onto one model neuron, all recorded on the same patch. DSi for ON-OFF cells are higher than DSi for SPN, indicating non direction selectivity postsynaptic neuron.

d) Five neurons synapsing onto one model neuron. DSi SPN=0.38. All the ON-OFF DSRGCs have DSi DSRGC > DSi SPN.

ON DSRGCs convergent inputs sharpens direction selectivity at the postsynaptic target.

We combined a pair of two recorded ON DSRGCs which send simultaneous convergent excitatory synaptic inputs to the same simulated postsynaptic neuron. The two ON DSRGCs have different indices of selectivity. For the first cell DSi1= 0.34 while for the second cell in the pair DSi2=0.30.We found that at the SPN the degree of sharpening in direction selectivity is slightly improved compared with monosynaptic scenario. Fig 8 show iS values for different gmaxe values a) when the degree of sharpening at SPN (DSi SPN) is compared with first ON DSRGC (with DSi1) and in b) comparing with the second cell (with DSi2). Maximum of the degree of sharpening achieved already for gmaxe=0.06 uS, is iS=1.54 at the SPN level while in monosynaptic mechanism (Fig4a) a maximum of sharpening was iS= 1.41 (obtained at one of the cells for gmaxe =0.07 uS). Fig8 show also the fact that a sharpening at SPN is obtained for a wider range of parameter gmaxe. Combining two ON-DSRGCs we found an improvement in signaling direction of stimulus at postsynaptic target.

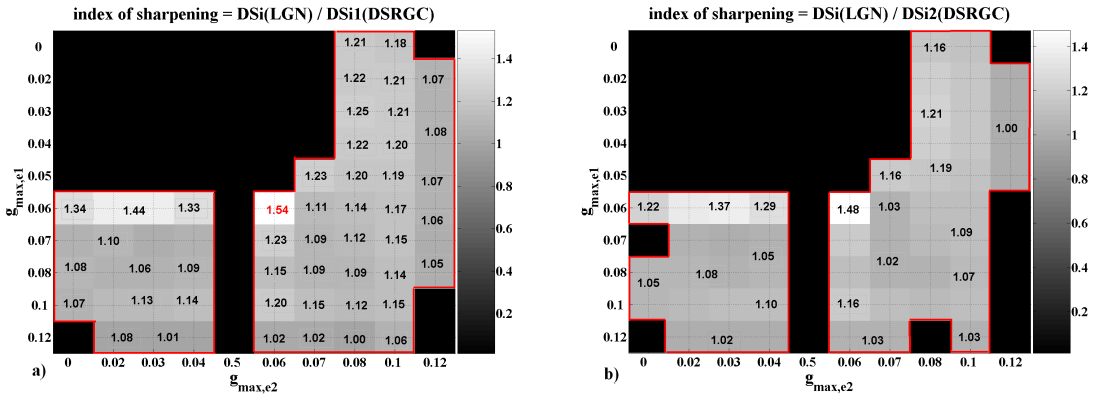

Fig8 Sharpening in direction selectivity obtained when considering a pair of two ON DSRGCs

a) Index of sharpening is obtained by dividing DSi SPN at DSi of the first cell in the pair which has DSi1=0.34. In this case iS reaches at maximum 1.54 a higher value than 1.41 which was achieved at maximum for one cell in monosynaptic mechanism. It is also obvious that for a larger domain of gmaxe values sharpening is obtained in polysynaptic mechanism.

b) iS for the second cell in the pair is at maximum 1.48 still higher than monosynaptic case. In this situation iS is obtained by dividing DSi SPN at DSi of the second cell in the pair DSi2=0.30.

Discussions

We sought a simple approach to investigate sharpening in direction selectivity at the output of rabbit retina. In this sense we used a simple model that proved to successfully describe retinogeniculate synaptic transmission in cat (Casti 2008 and primates (Carandini 2007) based on simple summation of EPSPs generated from recorded retinal spike trains followed by a threshold mechanism to generate AP at postsynaptic counterpart.

Monosynaptic Input. Intrinsic presynaptic property of ON-OFF DSRGC

In 2007 Sincich et al. have demonstrated that every spike within a burst at LGN neurons is generated by EPSP provoked by a retinal spike. In this logic there are a few chances that more than one AP at SPN to be evoked by a single EPSP. That further implies that if there is an AP at SPN it is due to at least one EPSP. Consequently, during boats of rapid firing activity there are higher chances to provoke more APs at SPN. Our results show the same. Burst-like activity at preferred direction was responsible for provoking a higher number of APs at SPN than at the intermediary directions (and thus sharpening directional tuning). Additionally they show that LGN neurons fired only if two EPSPs arrived sufficiently close in time. We found for all tested ON-OFF DSRGCs burst-like activity tuned at preferred direction, substantially higher than for ON DSRGCs. We therefore suggest that at preferred direction ON-OFF cells have a higher probability to successfully elicit an AP at postsynaptic target and thus to enhance the degree of direction selectivity.

The degree of sharpening could be predicted presynaptically at ON OFF DSRGCs by evaluating burst tuning for different directions of stimulus movement. Indeed, at the synaptic strength that evoked a maximum of sharpening in direction selectivity, we found that selectivity index for burst firing at ON-OFF DSRGC closely matched selectivity index of SPN for firing rate.

Polysynaptic input. Difference between ON-OFF AND ON DS cells

In our simulations we found that monosynaptic excitatory input alone led to a better signaling direction of stimulus motion at SPN for a wide range of synaptic strength. Excitatory synaptic conductance was reported as crucial in retinogeniculate transmission models (Casti et al. 2007, Carandini et al. 2007). It is well known that more than one retinal ganglion cells project to the same postsynaptic target (Regehr et al. 2005) but only one cell will mainly drive it. We checked polysynaptic mechanism and we found that the degree of sharpening at SPN was not improved comparing to monosynaptic connectivity.

Inhibition may also contributing to sharpening of directional tuning (Levick 1969) but in our simple approach inhibition did not dramatically change the degree of directional tuning at SPN (a minor role of inhibition was reported by Casti 2007 in a similar approach manner). It seems that rapid firing activity at ON OFF DSRGCs during presentation of stimulus moving at preferred direction is the key in narrowing the tuning curves at SPN. Indeed, we found significantly less similar property of burst-like activity in ON DSRGCs and artificial spike trains for which sharpening in direction selectivity at SPN was weak. Presumably for ON DSRGCs polysynaptic

mechanism (Soodak et al. 1988) is more likely to sharpen directional tuning at the postsynaptic target, while for ON-OFF DSRGCs polysynaptic inputs have had less efficacy.

Research efforts dedicated to ON DSRGCs have revealed that ON DS cells comprise three physiological subtypes distinguished by their preferred directions, each corresponding to upward, downward, or temporal-to-nasal motion in the visual field (Oyster 1968). The same preferred directions are present in the neurons of AOS nuclei (medial, lateral and dorsal). Other many response properties of AOS neurons (i.e. selectivity for stimulus velocity and size) are similar to those of ON-DS RGCs and thus this type of RGC is presumably the predominant if not the only input to the AOS neurons (Soodak et al. 1988, Oyster 1972, Amthor et al 1989a) initiating the optokinetic reflex.

It is suggested that AOS neurons' large directionally selective receptive fields could be formed from convergent inputs from ON-DS RGCs (Soodak et al.1988). We found that two ON DSRGCs exhibiting correlated and synchronous firing activity (Ackert et al. 2006) sending excitatory synaptic input on the same postsynaptic neuron will contribute to a better degree of direction selectivity at the target. It is interesting to further investigate if a larger number of converging ON DSRGCs (Soodak et al. 1988) could give rise to a more significant sharpening in direction selectivity at AOS neurons.

4. Descriptive Model for ON-OFF DSRGC receptive field characterization

Receptive field characterization is an important step in investigating basic properties of a visual neuron response. The center surround organization of retinal ganglion cells (and LGN neurons as well) explained many of their visual response properties. It is already well known that their behavior is well described by linear filtering of the stimulus presented over the receptive field. However, retinal ganglion cells present a wide variety of response characteristics some of them being nonlinear, among which is direction selectivity. To account for direction selectivity, the organization of receptive field must be treated as inseparable in space and time. Spatial structure of the receptive field reverses over time, so that the center and surround regions change their signs as the time advances. The key for inseparability is that there is a difference between the speeds at which they reverse their sign. The center of the receptive field of the ON-OFF DSRGCs changes the sign faster than the surround.

For the case of separable space time receptive fields the center surround organization of an ON-OFF RGC is very well captured by a difference of two Gaussians (DOG).

$$D(x,y) = \frac{1}{2\pi\sigma_c{}^2} e^{((-x^2+y^2)/2\pi\sigma_c{}^2)} - \frac{B}{2\pi\sigma_s{}^2} e^{((-x^2+y^2)/2\pi\sigma_s{}^2)}$$

Eq.1 Difference of two Gaussians fitted for a non-directional selective ON-OFF DSRGC extracellularly recorded.

The center of the RF was placed at x=y=0, the two Gaussians representing the center and the surround, respectively. The size of the center and the surround is modeled by σ_c and σ_s respectively, while B represents the strength of the surround of the receptive field.

Fig. 1 and Fig. 2 show an example of separable receptive field of an ON-OFF non-direction selective recorded in rabbit retina during a stimulus presentation consisting in grating bars moving in a particular direction for 12 seconds.

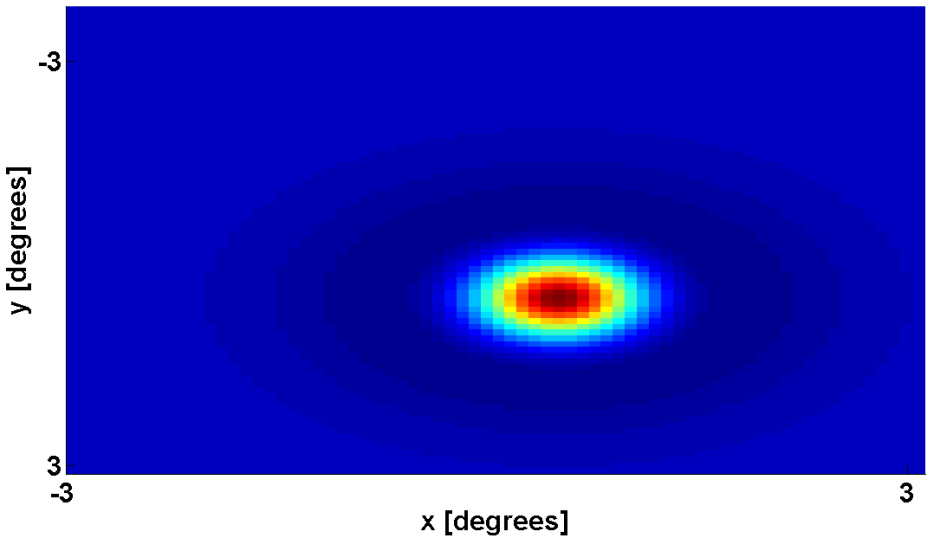

Fig. 1 The separable center-surround spatial receptive field structure characterized by a central ON region and a surrounding OFF region. Data recorded for an ON-OFF RGC after a 12 s grating bar stimulus presentation.

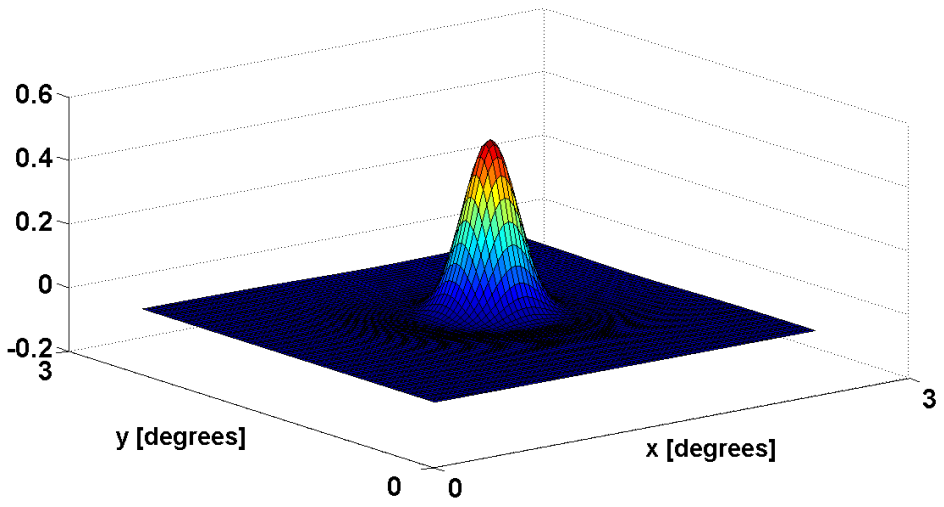

Fig.2 A fit of the receptive field shown in Fig. 1 using (Eq.1) a difference of Gaussians function, with σ_c=0.3^o, σ_s=1.2^o and B=2.

It is suggested that direction selectivity can be described by linear spatiotemporal RF structure of ON-OFF DSRGCs. These cells with RF profile tilted in space-time domain are expected to show a preference for a direction of motion while cells with separable space time RF would not. However, linear prediction usually underestimates the degree of direction selectivity measured from the recorded spike trains as response to a moving stimulus such as drifting gratings. These differences can be diminished if we take into account some nonlinearity in the cell's response. The nonlinearities presumably will increase the degree of the direction selectivity modeled by linear spatiotemporal RF structure. We used in the following the white noise analysis and reverse correlation technique to build a descriptive model to characterize the spatio-temporal structure of ON-OFF DSRGCS. To successfully describe the formation of the receptive field we add static

nonlinearities which explain most of the dynamic changes in space and time of the ON-OFF DSRGCs receptive fields.

The main steps we used are:

1. Build white noise stimulus

2. Record from ON-OFF DSRGCs stimulated with white noise stimulus

3. Calculate the STA in response to white noise stimulus and extract the kernel

4. Find the optimal kernel by adjusting the estimated firing rate to the recorded firing rate

5. Record data with new stimulus, consisting drifting grating bars (as described in Ch. 3 Methods)

6. Construct the linear model

7. Add static non-linearities

8. Compare predicted with recorded data

Mapping receptive fields of ON-OFF DSRGCs

Neurons in retina operate on visual stimuli mostly in a linear fashion. However, some of retinal ganglion cells responses are not entirely linear. One of the response property which involves non-linearities is represented by direction selectivity. To account for nonlinearities we propose a model in which model neurons have a linear receptive field, and static nonlinearities. To test this model we recorded responses from ON-OFF DSRGCs of rabbit retina. We estimate model parameters from a basic set of measurements using white noise stimulus and show that the model can accurately predict responses new stimuli.

To adequately describe how a neuron processes the visual image, one must characterize its RF in the joint space-time domain. We used the white noise stimulation combined with Wiener kernel analysis to characterize neurons with arbitrarily complex nonlinear response properties. White noise stimulus has a flat power spectrum and has several advantages: the stochastic, highly interleaved stimulus spans a wide range of visual inputs, is relatively robust to fluctuations in responsivity, avoids adaptation to strong or prolonged stimuli and is well suited to simultaneous measurements from multiple neurons.

1. **White Noise Stimulus and STA**

A white noise technique is presented for estimating the response properties of spiking visual system neurons. The technique is robust and appropriate to simultaneous recordings from multiple neurons.

As we already mentioned white noise stimulus has the defining characteristic that its value at any time is uncorrelated with its value at any other time (Fig.3).

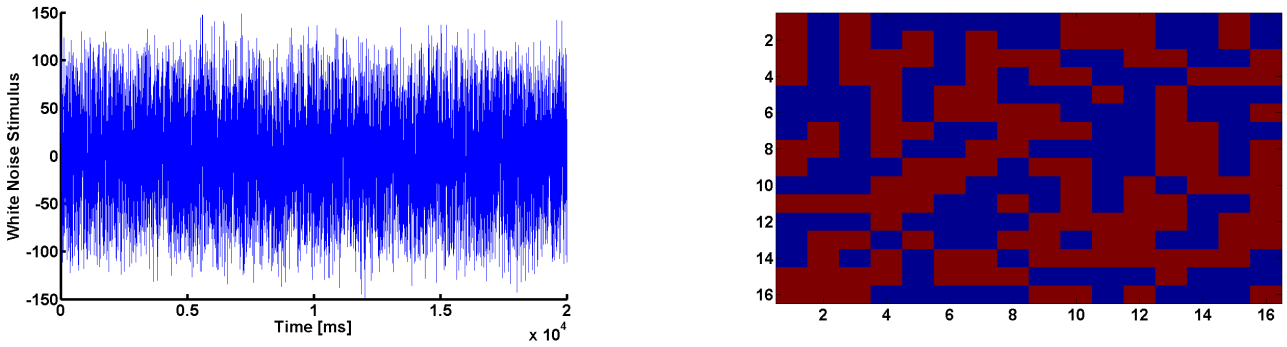

Fig. 3 Frequency and spatial arrangement of binary white noise stimulus updated every 20 ms used for the recorded data from ON-OFF DSRGCs.

For white noise stimulus the autocorrelation function is 0 in the range –T/2 <τ < T/2 except when τ=0 and for this value $Q_{ss} = \sigma_s^2 \delta(\tau)$, where σ_s which has the units of stimulus times the square root of unit time, reflects the magnitude of the variability of the white noise.

The spike triggered average is related to the reverse correlation function as discussed already by :

$C(\tau) = \frac{n}{T} Q_{rs}(-\tau)$, and represents the average value of the stimulus a time interval tau before a spike is fired, and thus is proportional to the correlation of the firing rate with the stimulus at

preceding times. Fig. 4 and Fig.5 show the STA calculated after white noise stimulus presentation from two ON-OFF DSRGCs recorded extracellularly from the same retinal patch. As can be noticed around 100-120 ms before a spike was triggered we found the maximum of the firing rate-stimulus correlation. Fig. 6 shows the receptive field structure at maximum correlation for one of the recorded neurons.

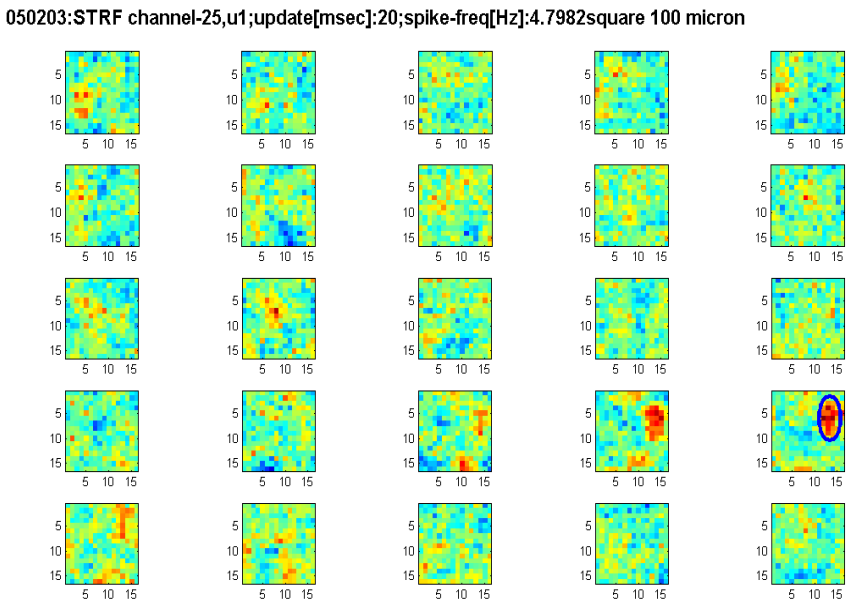

Fig.4 Evolution of STA for one ON-OFF DSRGC recorded after white noise stimulus presentation. At 120 ms before a spike was fired STA has a maximum. Before 120 ms the receptive field is changing polarity. Sooner than 120 ms the stimulus has little or no influence for the receptive field.

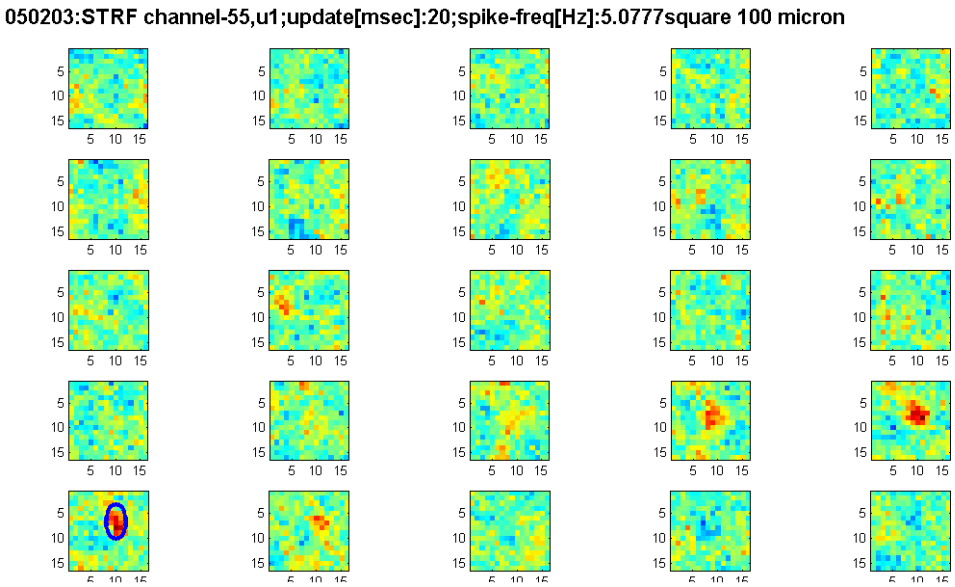

Fig. 5 Evolution of STA for another ON-OFF DSRGC using white noise stimulus. Maximum correlation between stimulus and neural response is found at 100 ms before a spike is fired.

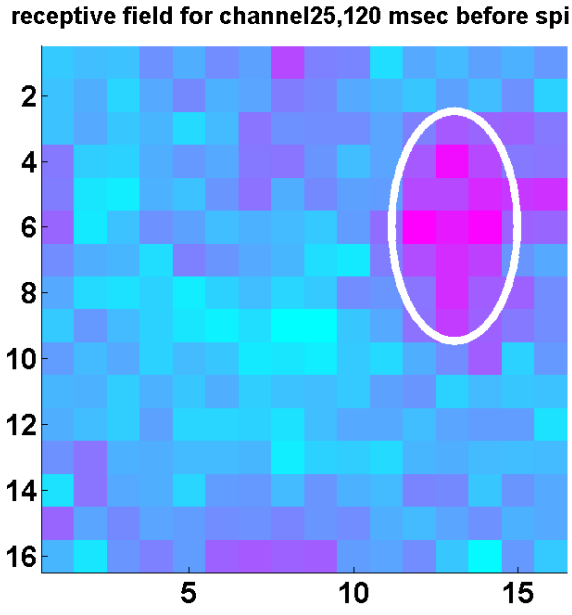

Fig. 6 Receptive field of one ON-OFF DSRGC mapped with noise and STA described in Fig.4.

As we have seen the best kernel which describe the receptive field organization in response to white noise stimulus is related to STA by the relation:

$$D(\tau) = \frac{Q_{rs}(-\tau)}{\sigma_s^2} = \frac{n}{T}\frac{C(\tau)}{\sigma_s^2}$$

For each of the recorded ON-OFF DSRGC we calculated the STA and the optimal kernel as above described. The spatial receptive field was defined as the average stimulus that preceded each spike in the range up to 300 ms. The lengths and widths of the subfields were quantified by fitting the spatial receptive fields, RF(X,Y), to elliptical Gaussians :

$$D_{x,y}cen, sur = A * \exp(-(a*(x-x_0)^2 + 2b*(x-x_0)*(y-y_0) + c*(y-y_0)^2))$$

Where :

a cen,sur = cos(theta)^2/2/sigma_x^2 + sin(theta)^2/2/sigma_y^2;

b cen,sur = -sin(2*theta)/4/sigma_x^2 + sin(2*theta)/4/sigma_y^2 ;

c cen,sur = sin(theta)^2/2/sigma_x^2 + cos(theta)^2/2/sigma_y^2;

All parameters describing the spatial structure - magnitude, orientation, elongation, eccentricity, were fixed by fitting procedure between white noise recorded data and predicted data as shown for example in Fig. 7.

To account for the direction selectivity we constructed the receptive field as being non-separable in the space-time domain. To accomplish this we multiplied the center and surround (ON and OFF subfields) with separate functions of time, which describe the time course of the receptive fields separately for ON and OFF regions. Because of the difference between time course of the center and of the surround regions, the space time receptive field is not separable, although the center and the surround components are individually separable.

$$D_t cen, sur = \alpha^2 cen, sur * \tau * \exp(-\alpha cen, sur * \tau) - \beta^2 cen, sur * \tau * \exp(-\beta cen, sur * \tau)$$

The parameters α cen,sur control the latency of the response in the center and the surround regions, and β cen,sur affect the time of the reversal.

The complete form of our space-time optimal kernel is thus (Fig. 8 and Fig. 9):

$$D_{xyt} = D_{xy} cen * D_t cen - D_{xy} sur * D_t sur$$

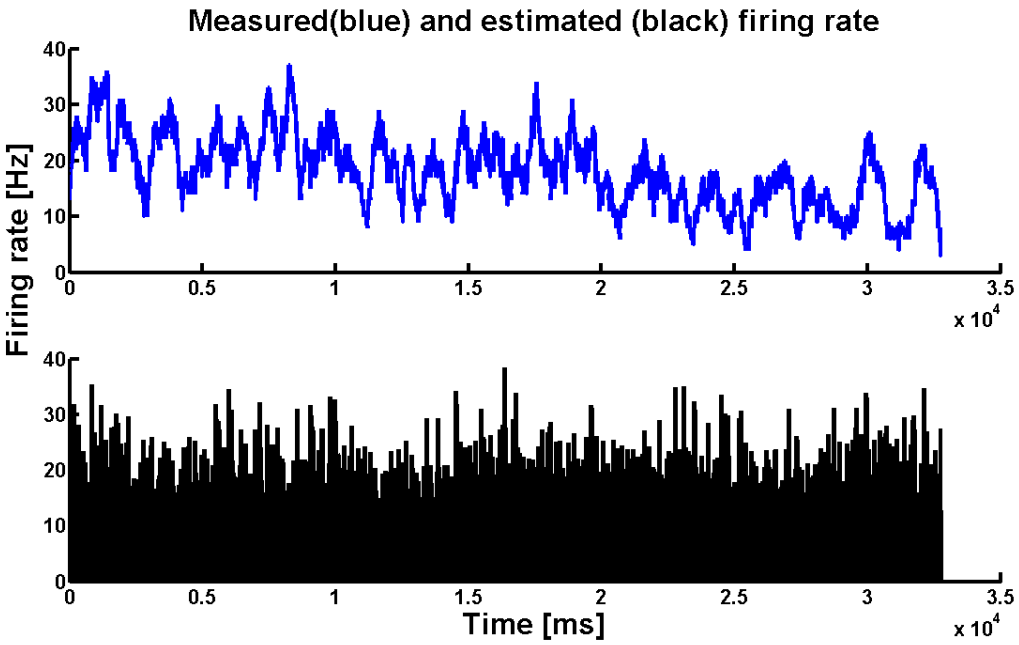

Fig. 7 Comparison of measured and estimated firing rates of one ON-OFF DSRGC using white noise stimulus and reverse correlation technique. The timing and magnitude of recorded data are accurately predicted by model.

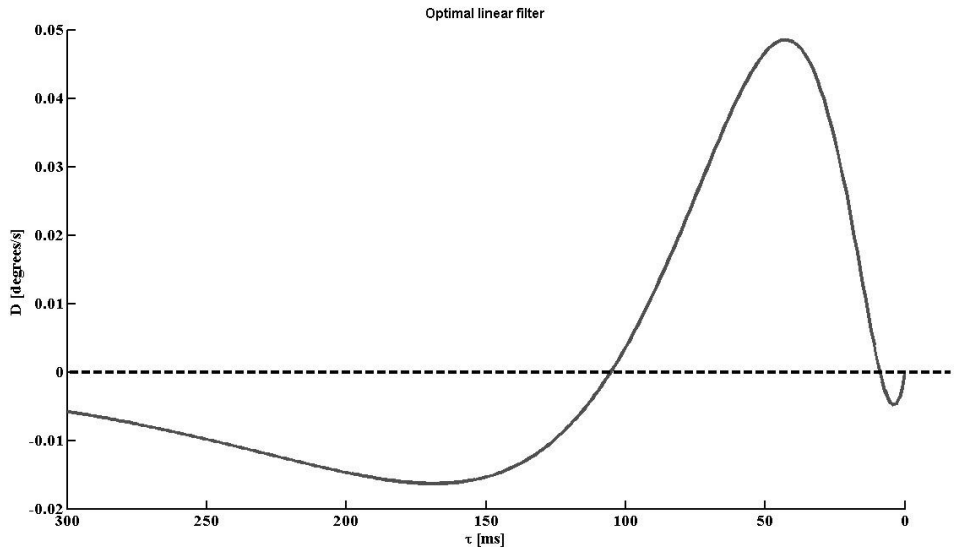

Fig. 8 Temporal course of optimal kernel inferred from best fitting recorded data with predicted data. Both ON and OFF structures are comprised. With 60-80 ms before a spike is fired the correlation between stimulus and firing rate is maximum. Time course of receptive center shows how the transformation between ON and OFF is produced.

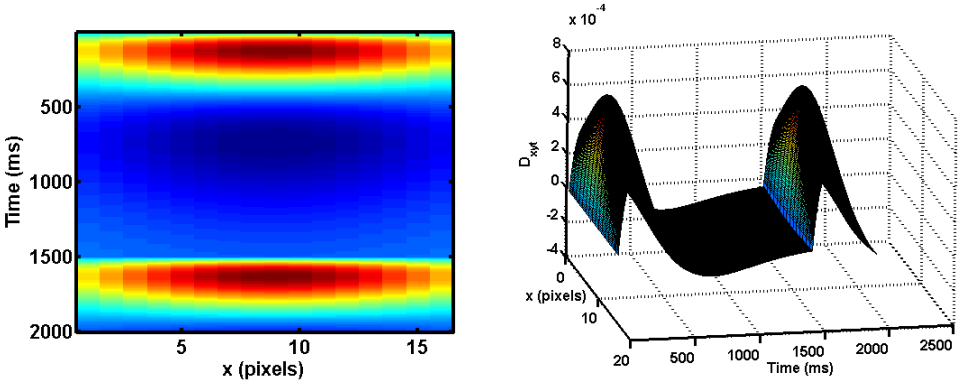

Fig. 9 Receptive field of ON-OFF DSRGC. Left. The center surround spatial structure of the receptive field. As time increases the ON OFF regions change the sign. Right. Optimal kernel fitted to match the receptive field transformations.

2. **Drifting grating bars stimulus**

To test the model prediction we used a novel stimulus consisting in drifting bars moving in different directions 45 degrees apart:

$I_{xyt} = A*\cos(k*x*\cos(\theta)+k*y*\sin(\theta)-\varphi)*\cos(\omega*t)$

The intensity of the stimulus oscillates in both, space and time. At any fixed time, it oscillates in direction perpendicular to the orientation angle (θ) as a function of position, with wavelength $2*\pi/k$. At any fixed position, it oscillates in time with period $2* \pi / \omega$ (Fig. 10). Amplitude of the signal intensity is controlled by parameter A, while drifting phase is given by angle φ.

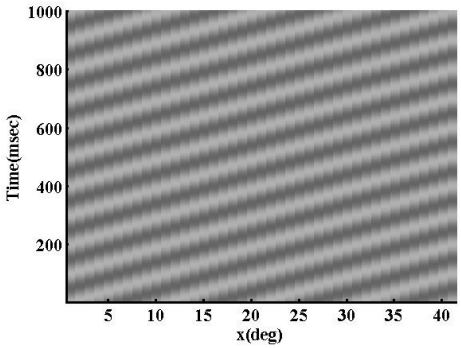

Fig. 10 Grating bars stimulus – space-time evolution. The x location of the dark and light bars moves to the right as the time progresses upward, representing the motion of the gratings

3. **Linear Non-linear model to predict direction selectivity**

The kernel needed to describe direction selectivity of ON-OFF DSRGC visual response property was first extracted using white noise stimulus as described above. We then used grating bars stimulus and construct a complete model to predict the direction selectivity of the recorded cells. The optimal kernel produces an estimate of the firing rate that is a linear filter of the stimulus. In order to deal with some of the deficiencies of the linear prediction we added a nonlinear function (F(L)) of the linearly filtered stimulus (Fig. 11). F is a function of the linear filter value instantaneously evaluated at the time of the rate estimation. Once that F is bounded from above and below, the estimated firing rate will never be negative or unrealistically large. Static nonlinearities are used to introduce both firing thresholds and saturation into estimates of neural responses. The model of spike trains evoked by our stimulus has been constructed by using firing rate estimate of equation bellow, to drive a Poisson process of spike generation.

$$L(t) = \int_0^\infty d\tau D_{xyt}(\tau) I_{xyt}(t-\tau);\ rest(t) = r_0 + F(L(t))$$

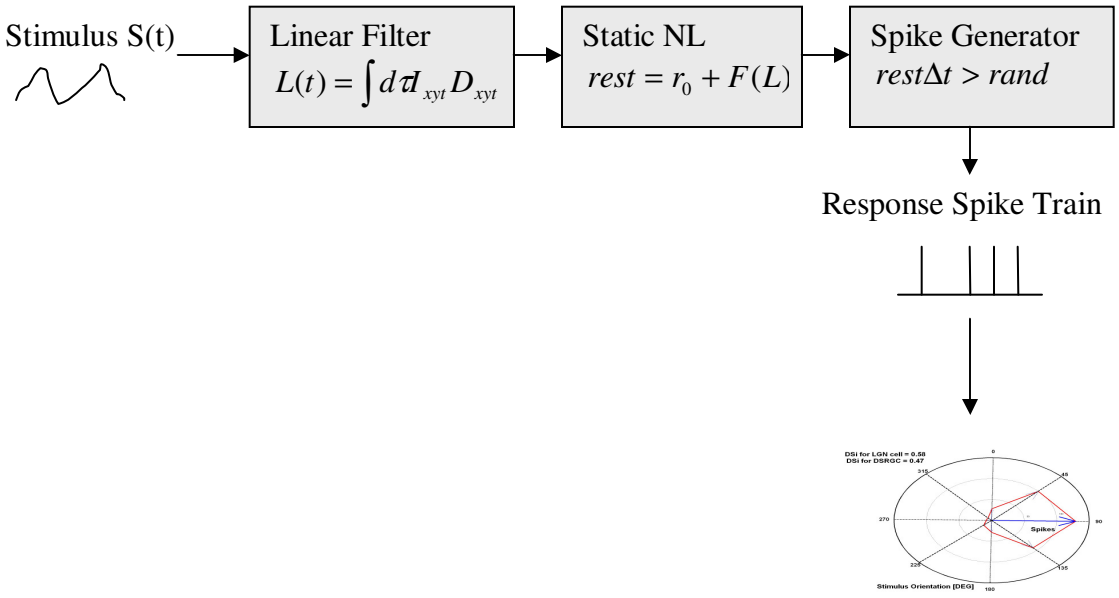

Fig. 11 Linear – Non-linear model to simulate spiking responses to stimuli. The integral of the stimulus I_{xyt} times the optimal kernel D_{xyt} is first computed as being the linear filter. The estimated firing rate is the background firing rate plus a nonlinear function of the output of the linear filter calculation. Finally, the estimated firing rate is used to drive a Poisson process to generate the predicted spike trains. Ultimately, the DSi for the predicted activity is indicating the predicted degree of direction selectivity.

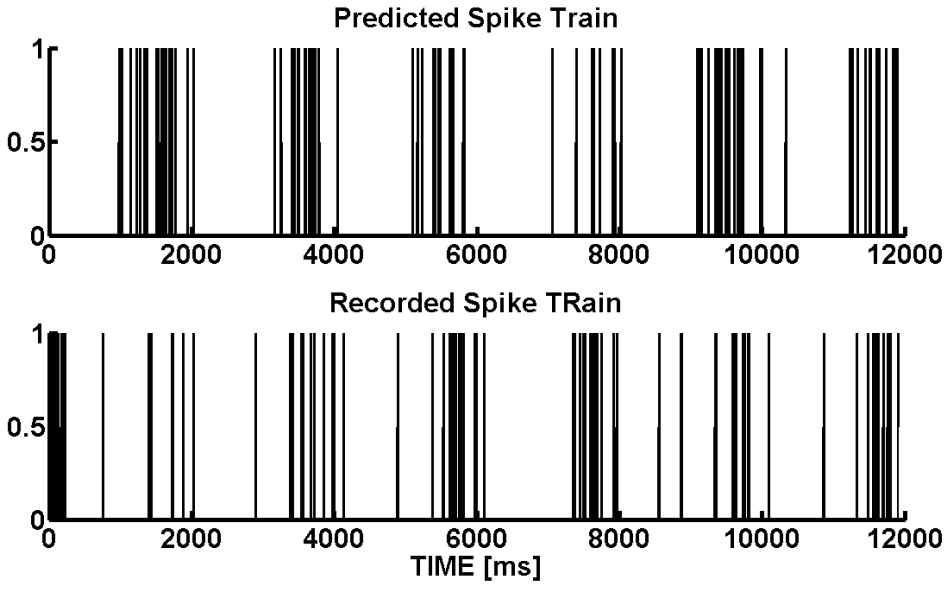

Fig.12 Comparison between predicted and recorded spike trains.

Fig. 12 show us an example of predicted spike trains which reproduce the recorded spike train of an ON-OFF DSRGC stimulated for 12 s with a drifting grating bars stimulus. In the next step we calculated the index of selectivity in order compare the degree of directional tuning for the recorded and predicted spike trains. Remarkably, as seen in Fig. 14, the degree of selectivity and the direction of selectivity were accurately predicted. The index of selectivity DSi for the predicted data was DSi =0.48 and the index of selectivity obtained for recorded ON-OFF DSRGC was DSi=0.49. The preferred direction was also accurately indicated by our model (90 degrees for the example).

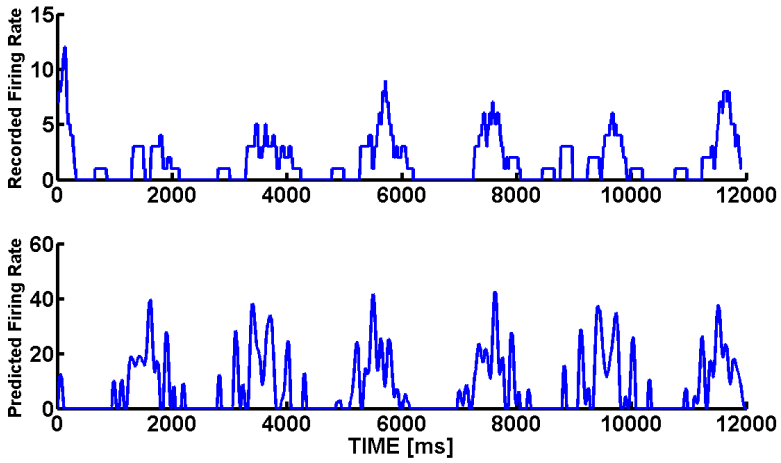

Fig. 13 Recorded and predicted firing rates. The lower plot is the rate predicted by integrating the product of stimulus intensity and a linear filter followed by a function applied over the linear filter. The upper plot show the recorded data.

Ultimately, the goal of this work is to present an accurate model for direction selectivity in retina based on receptive field characterization. The fact that firing rate of the predicted data did not match 100% the recorded data can be explained taking into account different aspects (i.e. higher order of nonlinearities, spike generator, etc) but our scope was to build a model which accurately can indicate the degree of direction selectivity and the direction of stimulus movement.

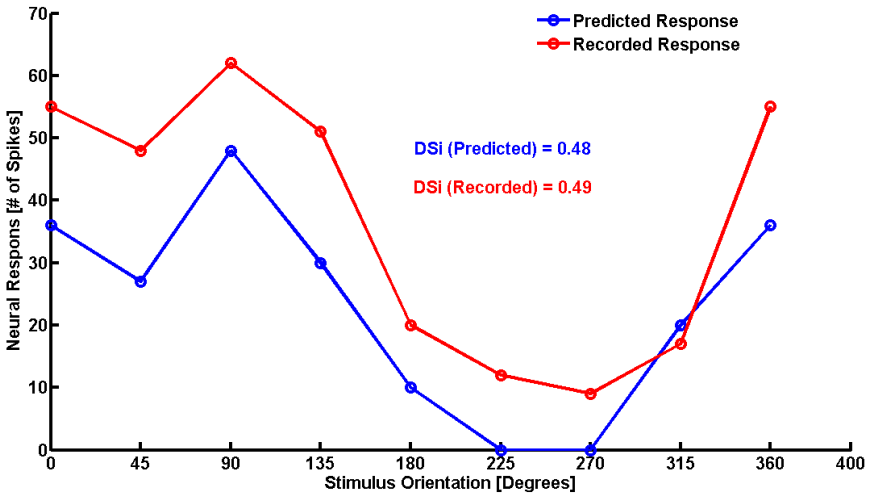

Fig. 14 Predicted and recorded tuning curves and indexes of selectivity.

Discussions

For a majority of cells, the spatial structure of the RF changes as a function of time; thus, these RFs can be effectively characterized only in the space-time domain. Thus, to describe how a neuron processes the visual image, one must characterize its RF in the joint space-time domain. Space-time separability means that the three-dimensional RF, RF(x,y,t), can be described as the product of a spatial structure, S(x,y), and a temporal structure, D(t) (i.e., RF(x,y,t) = S(x,y) x D(t)). For these cells, traditional methods of RF mapping (Fig.1 and Fig.2), which average responses over time, will not provide an accurate map of the RF. This inseparability is clearly illustrated by examining the spatiotemporal RFs of directional selective cells (Fig. 9. a,b).

The temporal sequence of RF profiles in Fig. 9 a presented in a movie sequence show RF subregions apparently moving in time. However, the spatial structure of the RF remains approximately the same as time progresses. This characteristic form of space-time inseparability has implications for understanding motion selectivity.

Because the x-t profile provides an accurate description of the visual response properties of most DS cells, we describe the spatiotemporal RF structure by making linear predictions of the response of a DS cell to a conventional stimulus. Fig. 13 shows predicted responses of a ON-OFF DSRGC with a space-time inseparable RF.

The essence of this approach is to obtain a complete description of the input-output relationship of a neuron (i.e., its RF profile) by testing it with a rich, spatiotemporal stimulus (i.e. white noise). By extending the traditional description of visual RFs into the joint space-time (*x*-*y*-*t*) domain, research efforts related to study of RF dynamics have provided new information about mechanisms of visual information processing in the early visual system pathways. A prominent conclusion of these studies is that the RF must be treated as a spatiotemporal entity.

In principle, white-noise analysis can provide a complete characterization of the behavior of any nonlinear system. However, it is worth noting that successful application of these models has thus far been limited to the study of neurons in the early portions of the visual pathway, for which response properties are well described in terms of first- and second-order correlations. For neurons in higher visual areas, the increasing complexity of RF organization is likely to demand the measurement of higher-order correlations and consequently, longer recording times. The method we applied take into account nonlinearities that are present in most neurons, such as spike threshold and saturation. These nonlinearities stepped beyond principles of standard linear systems analysis.

Moreover, the characteristic parameters of the static nonlinear model advantageously describe the relative sensitivity of the neuron to different aspects of the stimulus.

The model we implemented here tries to explain the direction selectivity based on a basic property of the direction selective ON-OFF retinal ganglion cells, namely, the space-time inseparability. We have shown how using white noise stimulus and reverse correlation, we inferred the optimal kernel and used it to build a linear filter in order to predict neuronal responses to new stimulus. This kernel has the particularity that it describes the RF structure in both, space and time together. To enhance the predicted degree of directional tuning we used static nonlinearities.

As our ultimate goal is to accurately predict the directional tuning, we have shown using this model and recorded data from ON-OFF DSRGC (using two different stimuli) that based on space-time inseparability of the DSRGCs' RF one can predict the preferred direction of a DS cell.
The model must be improved further and tested using for example another important DS cell type in the retina, namely ON DSRGC. One next step is also to test if the degree of sharpening at the postsynaptic target of these cells can be described using this method.

References

Ackert, J. M., Wu, S. H., Lee,J. C., Abrams, J., Hu, E. H., Perlman, I., and
Bloomfield, S. A. Light-Induced Changes in Spike Synchronization between Coupled ON Direction Selective Ganglion Cells in the Mammalian Retina. The Journal of Neuroscience, April 19, 2006 • 26(16):4206–4215

Alitto, H. J., and Usrey, W. M. (2005). Dynamic properties of thalamic neurons for vision. Progress in Brain Research, 149, 83–90.

Amthor, F. R., Takahashi, E. S., and Oyster, C. W. (1989a). Morphologies of rabbit retinal ganglion cells with complex receptive fields. J. Comp. Neurol. 280(1), 97–121.

Barlow, H. B., Hill, R. M., and Levick, W. R. (1964). Retinal ganglion cells responding selectively to direction and speed of image motion in the rabbit. Journal of Physiology, 173, 377–407.

Barlow, H.B., and Levick, W.R. (1969). Changes in the maintained discharge with adaptation level in the cat retina. Journal of Physiology, 202, 699–718.

Berson D M, Retinal Ganglion Cell Types and Their Central Projections Brown University, Providence, RI, USA 2008 Elsevier Inc.

Blitz, D. M., and Regehr, W. G. (2003). Retinogeniculate synaptic properties controlling spike number and timing in relay neurons. Journal of Neurophysiology, 90(4), 2438–2450.

Blitz, D. M., and Regehr, W. G. (2005). Timing and specificity of feed-forward inhibition within the LGN. Neuron, 45(6), 917–928.

Buhl, E. H. and Peichl, L. (1986). Morphology of rabbit retinal ganglion cells projecting to the medial terminal nucleus of the accessory optic system. Journal of Comparative Neurology, 253(2), 163–174.

Carandini, M., Horton, J. C., Sincich, L. C. (2007).Thalamic filtering of retinal spike trains by postsynaptic summation, Journal of Vision, 7(14):20, 1–11.

Casti, A., Hayot, F., Xiao, Y., Kaplan E. (2008). A simple model of retina-LGN transmission, Journal of Computational Neuroscience, doi:10.1007/s10827-007-0053-7

Chen, C., and Regehr, W.G. (2000). Developmental remodeling of the retinogeniculate synapse. Neuron, 28, 955–966.

Chen, C., Blitz, D.M., and Regehr, W.G. (2002). Contributions of re-ceptor desensitization and saturation to plasticity at the retinogeni-culate synapse. Neuron, 33, 779–788.

Cleland, B. G., Lewick, W. R., Morstyn , R., Wagner, H. G. (1976). Lateral geniculate relay of slowly conducting retinal afferents to cat visual cortex, Journal of Physiology, 255, 299-320.

Chalupa, L. M. and Werner, J. S. (2003), Visual Neuroscience, Vol.1 chapter V. Subcortical Processing. (pp. 565-657), MIT Press.

Dann, J. F. and Buhl, E. H. 1987. Retinal ganglion cells projecting to the accessory optic system in the rat. Journal Comparative Neurology, 262(1), 141–158.

Dayan, P., and Abbott, L.F. (2001). Theoretical Neuroscience Computational and Mathematical Modeling of Neural Systems. MIT Press.

Devries, S. H. and Baylor, D. A. (1997). Mosaic arrangement of ganglion cell receptive fields in rabbit retina. J. Neurophysiol. 78(4), 2048–2060.

Grasse, K. L., Cynader, M. S., and Douglas, R. M. (1984). Alterations in response properties in the lateral and dorsal terminal nuclei of the cat accessory optic system following visual cortex lesions. Experimental Brain Research, 55(1), 69–80.

He, S. and Masland, R. H. (1998). ON direction-selective ganglion cells in the rabbit retina: dendritic morphology and pattern of fasciculation. Visual Neuroscience, 15(2), 369–375.

Hoffmann, K. P. and Distler, C. (1989). Quantitative analysis of visual receptive fields of neurons in nucleus of the optic tract and dorsal terminal nucleus of the accessory optic tract in macaque monkey. Journal of Neurophysiology, 62(2), 416–428.

Huberman, A. D., Wei W., Elstrott, J.,. Stafford, B. K., Feller, M. B., and Barres, B. A.(2009). Genetic Identification of an On-Off Direction- Selective Retinal Ganglion Cell Subtype Reveals a Layer-Specific Subcortical Map of Posterior Motion. DOI 10.1016/j.neuron.2009.04.014

Jack, J.J.B., Noble, D., Tsien, R.W. (1975, 1983) Electric current flow in excitable cells, 1st and 2nd edns. Oxford University Press, Oxford

Kim, I.J., Zhang, Y.,Yamagata, M., Meister, M., and Sanes, J.R.(2008). Molecular identification of a retinal cell type that responds to upward motion. *Nature* 452, 478-482

Levick, W. R., Oyster. C. W., Takahashi E. (1969). Rabbit Lateral Geniculate Nucleus: Sharpener of Directional Information, Science, New Series, Vol. 165, No. 3894, 712-714.

Levick, W. R. (1967). Receptive fields and trigger features of ganglion cells in the visual streak of the rabbits retina. Journal of Physiology, 188(3), 285–307.

Mustari, M. J. and Fuchs, A. F. (1989). Response properties of single units in the lateral terminal nucleus of the accessory optic system in the behaving primate. Journal of Neurophysiology, 61(6), 1207–1220.

Oyster CW (1968) The analysis of image motion by the rabbit retina. J Physiol 199: 613–635.

Paninski, L. (2004). Maximum likelihood estimation of cascade point-process neural encoding models. Network, 15(4), 243–262.

Peichl, L. (1991). Alpha ganglion cells in mammalian retinae: common properties, species differences, and some comments on other ganglion cells. Visual Neuroscience, 7(1-2), 155–169.

Pillow, J. W., Paninski, L., Uzzell, V. J., Simoncelli , E. P, and Chichilnisky, E. J. (2005). Prediction and decoding of retinal ganglion cell responses with a probabilistic spiking model. Journal of Neuroscience, 25(47), 11003–11013.

Pu, M. L., and Amthor, F. R. (1990b). Dendritic morphologies of retinal ganglion cells projecting to the nucleus of the optic tract in the rabbit. Journal of Comparative Neurology, 302(3), 657–674.

Rall, W. (1967). Distinguishing theoretical synaptic potentials computed for different soma-dendritic distributions of synaptic inputs. J Neurophys 30:1138-1168

Robert E. Soodak and John I. Simpson (1988). The Accessory Optic System of Rabbit. I. Basic Visual Response Properties. Journal of Neurophysiology.Vol. 60, No.6.

Rodieck, R. W. (1998). The First Steps in Seeing. Sinauer Associates, Inc.

Rodieck, R. W. and Watanabe, M. (1993). Survey of the morphology of macaque retinal ganglion cells that project to the pretectum, superior colliculus, and parvicellular laminae of the lateral geniculate nucleus. Journal of Comparative Neurology, 338(2), 289–303.

Roska, B., Molnar, A., and Werblin, F. S. (2006). Parallel processing in retinal ganglion cells: how integration of space-time patterns of excitation and inhibition form the spiking output. Journal of Neurophysiology, 95(6), 3810–3822.

Stanford, L. R. and Sherman, S. M. (1984). Structure/function relationships of retinal ganglion cells in the cat. Brain Research, 297(2), 381–386.

Taylor, W. R., and Vaney, D. I. (2002). Diverse Synaptic Mechanisms Generate Direction Selectivity in the Rabbit Retina, Journal of Neuroscience, 22(17), 7712–7720

Usrey, W.M., Reppas, J.B., & Reid, R.C.(1998). Paired-spike interactions and synaptic efficacy of retinal inputs to the thalamus. Nature,395(6700),384-387.

Usrey, W. M. (2002). Spike timing and visual processing in the retinogeniculocortical pathway, Philosophical Transactions of The Royal Society Lond. B Biological Sciences, 357, 1729–1737

van der Togt, C., van der Want, J., and Schmidt, M. (1993). Segregation of direction selective neurons and synaptic organization of inhibitory intranuclear connections in the medial terminal nucleus of the rat: an electrophysiological and immunoelectron microscopical study. Journal of Comparative Neurology, 338(2), 175–192.

Vaney, D. I., Levick, W. R., and Thibos, L. N. (1981a). Rabbit retinal ganglion cells. Receptive field classification and axonal conduction properties. Experimental Brain Research, 44(1), 27–33.

Vaney, D. I., Peichl, L., Wassle, H., and Illing, R. B. (1981b). Almost all ganglion cells in the rabbit retina project to the superior colliculus. Brain Research, 212(2), 447–453.

Wang, C. Robinson, David W., Chalupa, L.M. (1998). Calcium-Activated Potassium Conductances in Retinal Ganglion Cells of the Ferret. Journal of Neurophysiology, 79:151-158.

Wang, W., Jones, H. E., Andolina, I. M., Salt, T. E., and Sillito, A. M. (2006). Functional alignment of feedback effects from visual cortex to thalamus. Nature Neuroscience, 9 (10):1330-6.

Weng, S., Sun, W., and He, S. (2005). Identification of ON–OFF direction-selective ganglion cells in the mouse retina. Journal of Physiology, 562(Pt 3), 915–923.

Wörgötter , F., and Koch, C. (1991). A detailed model of the primary visual pathway in the cat: Comparison of afferent excitatory and intracortical inhibitory connection schemes for orientation selectivity. Journal of Neuroscience, 11(7), 1959–1979.

Yonehara K, Ishikane H, Sakuta H, Shintani T, Nakamura-Yonehara K, et al. (2009) Identification of Retinal Ganglion Cells and Their Projections Involved in Central Transmission of Information about Upward and Downward Image Motion. PLoS ONE 4(1): e4320. doi:10.1371/journal.pone.0004320

Zeck, G.M., Masland, R.H. (2007). Spike train signatures of retinal ganglion cell types. European Journal of Neuroscience, 26, 367-380.